SERVICE FAILURE ANALYSIS INVOLVING BRITTLE CRACKING MECHANISMS

Lt. W. F. Payne
Applications Laboratory

Modern air vehicles owe at least part of their impressive performance to the continual development of lighter weight structural components. These improved structures are achieved both by development of higher strength structural alloys and by more efficient use (higher design stresses) of available materials. The maximum yield strength of various systems employed in air weapons appears in table 1 as a function of time period since World War II and the continual increase in strength level with time is very apparent. Experience has shown that as the strength level of alloys increases, the susceptibility to various cracking and delayed fracture mechanisms also increases, thereby increasing risk of catastrophic service failures and reducing system reliability. Several common cracking mechanisms have frequently been encountered in service failure analysis, such as fatigue cracking, stress corrosion cracking, hydrogen embrittlement and stress alloying. The nature of these failure mechanisms is presumably distinct and characteristic of the specific mechanism. Hence, a review of present knowledge on these fracture characteristics should reveal how the cracking mechanism, operative in a given service failure, can be isolated and identified.

An attempt to accomplish a general review of fracture characteristics of the common cracking mechanisms with a view towards development of rigorous identification characteristics for use in service failure analysis is what we are attempting. Actual fracture surfaces from service failures are used throughout the discussion and two service failure experiences with high strength steel are treated in detail as an indication of present failure analysis capabilities with these alloys.

The reason for the pronounced concern regarding the cracking and delayed fracture mechanism in structural alloys is expressed in figure 1. Comparison of table 1 with figure 1 shows that the highest strength alloys employed at present are in the category of "notch sensitive" materials, that is, the high strength so desired by systems designers is rapidly lost in the presence of severe stress concentrations such as a crack. The cracking mechanisms previously mentioned, provide such cracks and the result is catastrophic service failures. It is important that service failure analysis promptly and accurately identify any of the cracking mechanisms occurring in hardware components, so that immediate corrective action may be taken to restore reliability. As we shall discover, present failure analysis occasionally fails to provide this capability.

FATIGUE

Fatigue failures are a problem of vital concern in aircraft structures which are subjected to pronounced aerodynamic and mechanical vibrations. The useful life of shafts, propellers and other rotating engine components, is frequently determined by resistance to fatigue cracking under cyclic loads. In military air vehicles, where maximum weight and limited lifetime designs are common, the useful limit of material strength is again determined by the resistance to fatigue cracking.

Fatigue may be defined as the phenomena leading to cracking under repeated or fluctuating stresses having a maximum value frequently much less than the static tensile

strength. For components subjected to cyclic stresses, designs usually incorporate large safety factors due to the difficulty of estimating the time required to initiate fatigue cracking and the difficulty of detecting fatigue cracking when it does occur. Because of such conservative design practice, a surprising amount of fatigue cracking can normally occur before the component is unable to support the imposed loads. The rotor blades of helicopters, for example, are a safety-of-flight component designed with large safety factors. Figure 2 shows the extensive fatigue cracking that was found in the main rotor blade during ground inspection of an H-34 helicopter. This isolated incident originated from an internal flaw (a large non-metallic inclusion) that escaped detection during quality control inspections and presumably the blade was successfully operating for many hours in the cracked condition. Figure 3 was taken from a 4-inch diameter propeller shaft where cracks as long as 22 inches were found during routine inspection.

There is a broad variety of loading profiles (combinations of stress-time-number of cycles) found in air weapon systems, depending upon the actual design and specific mission; and it is presumed that any fracture surface formed by fatigue cracking is a direct record of the specific loading pattern that caused the cracking. Using visual examinations, the conventional distinction in fatigue fracture appearances is between low stress–high cycle fatigue and high stress–low cycle fatigue. Figure 3 represents a classic case of trans-granular low stress–high cycle fatigue cracking and the origin can be seen at the surface (fatigue cracking is a surface cracking mechanism) as well as many circumferential rings or "breach marks" which represent changes in the loading profile revealed by the advancing crack front. Each zone of cracking represents fatigue crack progression during a relatively uniform loading profile.

For comparison, figure 4 shows the fracture surface of a structural panel where fatigue cracking occurred during a high stress—low cycle loading profile. The origin is again at the surface but the symmetrical progression markings have a much rougher texture and a different interpretation. Once fatigue cracking was permanently initiated by the rough machined surface, the maximum stresses in the loading profile were enough to initiate normal slow crack growth for a short time (the dark fracture areas) and this was followed by another stage of fatigue cracking (the shiny fracture areas). The next stress peak caused an additional slow crack progression stage, followed by another stage of fatigue cracking, and so forth. Thus, for this case of high stress—low cycle fatigue cracking, the symmetrical progression markings indicate actual changes in cracking mechanisms, from slow crack growth to fatigue cracking. The crack front was halted, in this example, as it advanced into a region where the stresses were too low to sustain fatigue cracking.

The most extensive damage from fatigue cracking (including catastrophic failure) has occurred when the problem of fatigue was not anticipated. Figure 5 shows the fractured surface of a high strength aluminum alloy skinplate with a fatigue crack originating at the bottom of a bolt hole. The presence of this small fatigue crack initiated a catastrophic failure of an entire wing during flight and resulted in loss of several lives and an aircraft worth several million dollars. The actual fatigue crack is far too small to be detected in real aircraft with present inspection capability and this structural design is an unreliable design -- the price paid for excessive notch sensitivity of an alloy for the given design. The problem of acoustical fatigue, first encountered with resonant vibration of turbine blades, is becoming more severe for structural skins with the increasing noise level of propulsion systems, and is a source of fatigue cracking occasionally overlooked.

Several years ago, an English paper (1) appeared showing photographs of replicas from fatigue fracture surfaces made with an electron microscope (magnifications of 13,000X and greater). It was immediately apparent that the electron microscope would become a

tremendously useful tool in fractography analysis. The fracture surface replicas shown in figure 6 are taken from low stress high cycle fatigue zones of several alloys subjected to a uniform loading profile (which would correspond to a single progression zone in the previous examples). A series of uniformly spaced nodes or striations are evident, apparently each representing a separate cracking stage, demonstrating the discontinuous nature of the transgranular fatigue cracking process.

The significant result from a fracture analysis standpoint is that measurement of the node separations should allow direct experimental measure of the stresses that existed during the cracking process in the structure.

When this direct stress measurement capability is fully developed, the engineer will no longer have to rely on the very approximate analytical stress analysis to help determine the reason for fatigue cracking problems in aircraft structures. Fracture patterns of several different metals are included to demonstrate the generality of the discontinuous cracking stages in various metals. The comparison between low stress—high cycle fatigue and high stress—low cycle fatigue is shown (for two specific samples) in figure 7. The high stress—low cycle fatigue cracking is evidently a very complicated process and direct reading of highly magnified fracture surfaces may not be possible. The Air Force has considerable interest in these recent fractography developments employing electron microscope techniques.

STRESS CORROSION CRACKING

This type of corrosion involves a complex interaction of sustained tension stress and corrosive attack that results in rapid cracking and the premature brittle failure of a normally ductile material. As a general phenomena, many metallic systems (from pure metals to commercial alloys) can be susceptible to stress corrosion cracking under certain environmental conditions. For example, the chemical process industry, with the variety of acids, chlorides and other active chemicals, frequently in hot aqueous solutions, has a long history of stress corrosion cracking problems in metallic structures, as well as general corrosion deterioration. Casual awareness of these and similar industrial problems, and the observation that laboratory stress corrosion cracking investigations are performed in apparently very corrosive media (such as boiling salt solution, with questionable correlation with normal atmospheric service conditions) has apparently led designers and materials engineers to the belief that the environment associated with normal atmospheric flight conditions is simply not corrosive enough to induce stress corrosion cracking in structural metals. Nothing could be farther from the truth. This is due to the increased susceptibility of high strength alloys, and often to the occurrence of unexpectedly severe corrosive conditions, while processing chemicals during manufacture, or salt on wet runways during winter deicing. The continuing occurrence of stress corrosion failures in service has frequently affected the operational reliability of many important weapons systems. The appearance of educational features by Alcoa (2) in national engineering publications indicates the importance of the problem. An example of structural damage in the outer cylinder of a main landing gear shown in figure 8 is attributed to stress corrosion cracking.

Three conditions are necessary for stress corrosion cracking 1) a corrosion susceptible material, 2) sustained tensile stresses, and 3) a corrosion reaction. The susceptibility comes from the same metallurgical reactions that produce the high strength properties of our present alloys. Figure 9 shows the relative susceptibility to stress corrosion cracking of the three primary grain directions (under controlled test conditions as

indicated); it is the transverse grain directions that are most susceptible to delayed cracking. Hence our service problems have mostly occurred due to transverse grain exposure in primary airframe components, such as forgings and extrusions, rather than sheet material. This fact emphasizes the need for grain flow control in forgings and extrusions for acceptable service behavior.

The sustained tensile stresses required for cracking to occur have, surprizingly enough, usually not been associated with the service stresses, but arise from residual stresses induced (and not controlled) during manufacturing processes. The main sources of these tensile stresses are:

1. Non-uniform cooling during the water quenching operation after precipitation hardening treatments.

2. Excessive mismatch with subsequent strains during fit-up and installation.

3. Exposure of tensile residual stresses by excessive machining operations following heat treatment. This serves to emphasize the necessity (not just the desirability) of optimum, well controlled manufacturing processing methods in order to improve the reliability of service hardware performance. Figure 10 shows the transverse residual stress pattern found in one of the landing gear cylinders following the precipitation and quenching treatment. Without proper control, a high level of residual stress is possible.

It is now apparent that if the transverse grain direction is exposed and the tensile residual stresses are allowed to become as severe as the previous example, then the third factor (the corrosive media) does not have to be very corrosive to cause stress corrosion cracking. That is precisely the case in many service failures. Figure 11 shows quite effectively the extent of cracking damage that can occur in normal aircraft environments, even though not operated in a salt air environment. In this case, the top section of the same type of landing gear shown earlier, the residual tensile stresses came from exposure by excessive machining of the I.D. surface of the residual tensile stress region formed during the quenching operation. The undesirable grain flow pattern in this area, shown in figure 11 results from excessive grain runout during the forging operations and has caused exposure of the most susceptible (short transverse) grain direction. The extensive cracking shows that service stresses were very low; in fact, the part never did fracture but the cracking was detected during an inspection.

ALUMINUM ALLOYS

Problems with the aluminum alloys have involved the high strength 20XX series (Al-Cu) and the 70XX series (Al-Fn-Mg-Cu) alloys. The Al-Cu alloys are susceptible because of precipitation of $CuAl_2$ in the grain boundaries, forming a copper-depleted zone near the grain boundary that is anodic to both the matrix of the grain and the $CuAl_2$. The 70XX series is susceptible apparently due to both grain boundary precipitation of $Mg_2\ Al_3$, which is anodic to the matrix, and formation of copper depleted zones during the $CuAl_2$ reaction. In at least one alloy (7075), susceptibility has been reduced considerably by an overaging heat treatment, with a slight loss in mechanical strength (roughly 6-10 percent).

The nature of stress corrosion cracking in aluminum is therefore intergranular as shown in figure 12, and this fact is frequently used to distinguish stress corrosion failure from fatigue cracking which is transgranular. The fracture surface of stress corrosion

failures is generally characterized by a brittle (intergranular) cracking zone progressing from an origin in a circular or semi-circular crack front, followed by the normal ductile fracture pattern of an overload failure, and this is shown in figure 13. Secondary intergranular cracking is frequently found in the microstructure near the fracture face especially when the corrosive environment is very active and is sometimes used as an identification criteria. However, such secondary cracking may not occur during cracking along very susceptible paths, such as the short transverse grain direction or in milder environments and is a sufficient but not necessary condition for identification of stress corrosion failures in aluminum (note the limited secondary cracking in figure 12).

The fractural landing gear cylinder shown in figure 14 was presumably exposed only to hydraulic fluid, possibly containing slight water contamination. Note that two distinct stress cracking zones are evident, separated by a zone of overload crack propagation which apparently was halted by reduction of the load acting on the landing gear. Experience shows that internal surface cracks such as the first cracking stage can be caused by processing chemicals reacting with high residual stresses. However, in this case, certainly the second stress corrosion cracking zone must be attributed to the impure hydraulic fluid, and perhaps the fluid was the "corrosive media" for the entire fracture.

The cracking shown in figure 15 demonstrates a frequently observed behavior in hardware failures - that conditions for stress corrosion cracking is actually associated with the existence of surface pits. Probably the stress concentration effects and altered (more severe) chemistry associated with a surface pit are the real cause for stress corrosion failures in many cases. Certainly, no stress corrosion susceptibility tests have been made in aluminum alloys that simulate this condition and this is an area where fundamental corrosion mechanism research is urgently needed.

Data on the susceptibility of various commercial aluminum alloys to stress corrosion cracking in accelerated laboratory tests has been published by Alcoa (2) (3). Although the basic mechanism causing susceptibility to stress corrosion cracking is at least empirically understood, it is not apparent why the susceptibility varies so drastically with grain direction. This aspect of the problem in aluminum alloys is presently under study at Armour Research Laboratories under ASD sponsorship (4).

HIGH STRENGTH STEEL ALLOYS

Stress corrosion in martensitic steels, such as the stainless AISI 400 series has been observed and studied for a number of years. However, it has only recently become apparent that our high strength low alloy martensitic steels are also susceptible to stress corrosion cracking. The data of Steigerwald (5) on the delayed strength of high strength steel containing cracks in the presence of the various environments, shown in table 1, indicates that the susceptibility becomes quite pronounced at the high strength levels. Preliminary test data published by Boeing (6) on stress corrosion susceptibility of certain steel alloys indicate that the transverse grain directions again have greater susceptibility to cracking. The mechanism of cracking in those alloys at the high strength levels (above 240,000 psi ultimate strength) is not known; this is another area where corrosion mechanism research is necessary. The nature of cracking in stress corrosion is intergranular along the prior austenite grain boundaries (although this is frequently difficult to determine with optical metallographic techniques) and the cracking frequently is accompanied by secondary cracking. The intergranular nature of stress corrosion

fractures in steel is more clearly shown in the electron microscope photograph of a fracture surface replica included as figure 16. Unfortunately, the relationship between the stress corrosion processes and the hydrogen embrittlement processes in low alloy steels is completely unresolved, and represents probably the most urgent area for additional corrosion research.

THE "THRESHOLD STRESS" DESIGN CONCEPT

Referring back to the stress corrosion susceptibility curve (figure 9), we see that a minimum stress exists for the occurrence of cracking (a "threshold stress") under the controlled test conditions. Far too frequently, it has been suggested that prevention of stress corrosion service problems can be accomplished by use of the threshold stress as design stress. This is an erroneous concept, and this approach is not adequate because the actual "threshold stress" varies with many factors, including grain direction, surface condition, the actual corrosive medium, the existence of stress concentrations, the length of exposure and the state of stress of the actual component (particularly the residual stress). Thus, a practical value of the "threshold stress" for design purposes is actually impossible to obtain. The practical answer to elimination of stress corrosion failures can be found only in competent design and fabrication and an understanding of the characteristics of the structural materials employed. This should result in (1) elimination of the exposure of very susceptible short transverse grain structure, (2) elimination of sustained tensile surface stresses (through control of residual stresses and installation stresses), (3) frequent use of protective coatings to include corrosive medium from the susceptible alloys and (4) the use of less susceptible alloys or improved heat treatments on present alloys.

STRESS ALLOYING

Another brittle failure mechanism involves the intergranular penetration of metals and alloys under stresses by liquid metals (stress alloying) and this difficulty has been encountered in steel alloys in the presence of metallic coatings with low melting points, such as cadmium. Failures with cadmium plated steel begin to occur as the temperature approaches 500°F, even though the melting point of cadmium is 611°F - the use of cadmium plated steel is not recommended for temperatures of 500°F and above. The fracture surfaces resulting from stress alloying with cadmium plating are shown in figure 17 and usually exhibit intergranular fracture surfaces with very little surface deformation and frequently evidence of cadmium on the fracture surface itself is evident.

A thorough study by Col. E. M. Kennedy (7) indicates that high temperature tensile, stress rupture and fatigue properties are seriously degraded in several heat treated high strength low alloy steels, and an example of this stress alloying effect is shown in figure 18. The shape of the curves is similar to that of other intergranular embrittlement mechanisms.

HYDROGEN EMBRITTLEMENT

In martensitic steels, the presence of hydrogen under the influence of sustained tensile stresses will result in delayed fractures, frequently in the presence of very little hydrogen if the sustained stresses are a large fraction of the yield strength. The kinetics of fracture are diffusion controlled and apparently related to diffusion of interstitially

dissolved hydrogen in the steel (such motion is relatively easy since the diameter of a hydrogen ion is 10^{-13} meters and the separation of atoms in the martensitic structure is on the order of 10^{-8} meters). Hydrogen embrittlement is part of the general condition of (BCC) metals by interstitial elements (which would include hydrogen, oxygen, carbon and nitrogen) and this embrittlement has been discussed by Trioano (8) (9) (10), Hill (11), Quist (12) and many others. Sensitivity of high strength steels to the presence of hydrogen, however, is far more pronounced than the other elements, and represents a serious limitation to reliable application of the high strength steels employed in present weapons systems.

One aviation company (13) has actually adopted the practice of empirically screening AISI 4340 steel shipments for susceptibility to hydrogen induced failure and restricts use of steel showing excessive hydrogen cracking susceptibility to a heat tested ultimate strength of 160 ksi. A discussion of the theories proposed to explain the pronounced effects is beyond the scope of this review, and are rather tentative in any case. The effects of hydrogen on mechanical properties is perhaps, the best way to show the behavior of hydrogen in steel. The influence of hydrogen on ductility and rupture strength of AISI 4340 is shown in figure 19; the adverse effects increase with strength level of the steel and with increasing time of sustained load. Figure 20 shows that the adverse effects increase somewhat with severity of the notch (stress concentration) and increase drastically with decreasing strain rate as higher strength levels are employed. The particular embrittlement condition described in figure 20 represents a material obviously unsatisfactory for a useful high strength structure.

A recent review of the extensive literature on the hydrogen embrittlement of high strength steels showed that investigators generally paid no attention to the fracture surfaces of experimental specimens, and the microstructural nature of cracking was not usually discussed, presumably due to the difficulty of rigorous metallographic interpretations. Corrosive investigations on the martensitic stainless steels (14) discovered that the cracking node changed from intergranular (under stress corrosion conditions) to transgranular (under hydrogen embrittlement conditions) and it was apparently assumed that a similar behavior was exhibited by the low alloy steels. However, an investigation by R. A. Davis (15) employing electron microscopy techniques shows that hydrogen embrittlement fractures in AISI 4340 and 4340M low alloy steel are definitely intergranular with respect to prior austenitic grain boundaries. Davis reported that the electron microscopy techniques were adequate to distinguish the subtle distinctions between stress corrosion and hydrogen embrittlement fractures (if this is true, it represents the only technique really capable of making such a distinction). A comparison of hydrogen embrittlement, stress corrosion and ductile fracture surfaces in steel is shown in figure 21; the differences between the two intergranular cracking mechanisms are seen to be subtle.

Occasional reference has been made to the presence of darking near the origin of hydrogen embrittlement fractures. (One recent paper referred to the dark fracture area as "typical of transgranular cracking.") It has been suggested that dissolved hydrogen might react with carbon to form methane, which diffuses to the fracture surface and decomposes leaving a dark carbon deposit. One of the alloy steel landing gear failures discussed later in the paper exhibits a dark origin but was identified by electron microscopy techniques as a stress corrosion failure. A great deal of research work remains to be done in the area of brittle characteristics of low alloy steels.

The original problem of hydrogen embrittlement failures occurred due to hydrogen penetration during cadmium plating operations on steel with ultimate strength of 180-200 ksi, and was presumably overcome by the use of baking treatments (up to 400°F for

several hours) to drive off the hydrogen absorbed during processing. For higher strength steel, a special cadmium plating process was developed which produced a porous coating of cadmium that allowed more complete removal of hydrogen during baking treatments. It finally became necessary to restrict the use of cadmium plating to steel with tensile strengths below 240 ksi.

However, as will be shown shortly, hydrogen embrittlement failures still occur, with the hydrogen arising from a variety of subtle sources, including process chemicals in production processes, lubricating oil used in machining, melting practice perhaps, atmospheric corrosion and possibly many sources we do not even realize.

MATERIAL QUALITY

While material quality is not a fracture mechanism itself, it frequently contributes to acceleration of failures by some of the mechanisms discussed in this paper. A condition which has frequently been noted on supposedly high quality steel forgings is shown in figure 23. The surface scale is an intergranular oxidation scale probably from heat treatment operations and the banding is a condition often detested in vacuum melted billets, as well as air melted stock. Experience would indicate that such surfaces may be the rule rather than the exception and perhaps must be expected on production components produced to existing specifications.

SUMMARY OF FRACTURE CHARACTERISTICS

It may be helpful to review the specific characteristics of the various fracture mechanisms which might be useful for the purposes of identification.

All cracking mechanisms occur without general deformation of the component, making detection difficult prior to total failure. Fatigue cracking (particularly low stress-high cycle fatigue) occurs from a surface in a transgranular mode and produces concentric arcs or "beach marks" which indicate the leading profile acting on the crack front. Use of electron microscopy techniques may allow direct experimental measurement of the stresses in the component prior to catastrophic failure. Stress corrosion cracking occurs from a surface in an intergranular mode in both aluminum and steel alloys, and generally produces a bright arc shaped zone of cracking prior to overload fracture. Secondary cracking is frequently present but not a satisfactory criteria for mechanism identification. Stress alloying occurs by intergranular penetration of a metal surface under stress by a liquid or highly viscous metal coating, such as cadmium or steel above 500°F; actual droplets of the penetrating metal are frequently visible. Hydrogen embrittlement of steel can be either intergranular (as in the low alloy steels) or transgranular (as in the high alloy steels). Rigorous criteria for fracture mechanism identification in low alloy steels are not presently available.

REVIEW OF SEVERAL SERVICE FAILURE ANALYSES

One recent service experience amply demonstrates the pronounced susceptibility to delayed cracking mechanisms in high strength materials - in this case, a landing gear axle forging made from AISI 4340 heat treated to 260-280 ksi ultimate strength. This gear was subjected to more qualification tests than any previous gear in Air Force history, and there was little doubt that the gear was capable of a full 8,000 cycles to

failure (conservative engineering practice specified a lifetime requirement of only 3,000 cycles to failure).

The first failure occurred when an internal surface gauge from a machining operation, which initiated crack growth and rapid fracture in the axle beam of the gear. Intergranular oxidation of the surface (0.0015 inches deep) tended to accelerate the crack initiation and growth stages. The pronounced notch sensitivity of steel at 260-280 ksi tensile strength will inevitably result in failures in the presence of surface damage and this failure was considered an isolated problem.

In early 1958, a second axle beam failure occurred and could not be explained by design faults or surface damage. The short transverse tensile specimens cut from the actual forgings indicated that the transverse ductility was of borderline aircraft quality by present standards (a short transverse ductility of greater than 20 percent reduction in area is desirable for 4340 forgings at the high strength levels.) The conclusion of marginal material was reached by the contractor.

Then in 1961 a failure occurred during a jacking operation after only a dozen landings and a picture of the broken axle beam is shown in figure 23 (a). Figure 23 (b) shows a view of the fracture face and the point of origin that occurred in the radius of the lower fillet. The primary cause of the failure was overheating during grinding operations (gringing "burns") resulting in severe surface damage shown in figure 24. A surface layer of untempered martensite (Rc55) up to 0.001 inch deep was noted in several places, with a subsurface layer of overtempered martensite (Rc36 or 170 ksi tensile strength) several thousands of an inch in depth (up to 0.010 inches in places) the base metal hardness was Rc51. Thus, the surface damage was capable of initiating a surface crack large enough to cause complete fracture of a 0.23-inch thick forging at a stress well below the yield strength.

By this point, a general rework program had been initiated to remove the surface damage, and qualification tests on the reworked gears indicated at least a 100 percent improvement in life. Out of five gears tested, four gears lasted between 16,000 - 18,000 cycles and a fifth gear, lasted 33,000 cycles to failure. This last result is typical of the improvements obtained with proper control of grain flow (orientation of the longitudinal grain flow in the direction of maximum load or in this case parallel to axis of the axle). The grain flow of the majority of the gears was random in the critical fillet area, with a coarse dendritic structure, which is far from the optimum forged condition, particularly for good transverse ductility. Note, however, that the expected life time was experimentally determined based on gears with random grain flow and the safety factor for lifetime of the reworked gears was about five. The gears again appeared satisfactory from an engineering standpoint.

In September, 1961, an axle fractured during normal take-off, but the fracture surfaces were damaged by impact and hindered the investigation. The fractured beam is shown in figure 25. Several intergranular cracks were noted near the fracture origin, up to .005 inches deep; see figure 26. Only one small area of surface damaged by grinding burns was found and this area was not associated with the failure. The intergranular cracking caused concern that stress corrosion cracking was present, which would indicate a fleet wide problem. The fillet surfaces had been thoroughly shot peened but were not coated and some minor surface pitting was evident with a 10X inspection. The possibility of hydrogen embrittlement, temper embrittlement from heat radiation effects during hard braking operations or corrosion fatigue were also suggested.

In November, 1961, both forward axles of one H beam catastrophically fractured one after the other while the crew was climbing into the aircraft (rather bad for the morale factor!) The estimated stress in the fillet was about 135 ksi at the time of initial failure. These gears had also been reworked to remove grinding burns and failure in both axles occurred in the high stress lower fillet area (see figure 27). The surface condition was uncoated shot peened steel but no serious rusting was evident. No evidence of grinding burns could be found in the primary failure and the secondary axle failure appeared to be a normal ductile failure caused by overload following the primary failure.

The fracture face of the primary failure is shown as figure 28 and close examination clearly shows the small origin capable of inducing catastrophic failure at this strength level. The close-up view of the origin shows a brittle surface crack about 1/64-inch deep by 1/16-inch long with a secondary progression ring roughly 3/32-inch deep by 11/64-inch long around the origin. The initial origin was initially interpreted as fatigue with the second stage progression probably due to crack growth under the sustained load of the fully fueled condition prior to anticipated take-off. In addition, small intergranular cracks were again noted in the primary fracture face and a secondary crack was detected at a point 1/8-inch apart from the primary crack (figure 29).

In view of the successful qualification tests for a full 3,000 cycles on many landing gears, which were believed to be of average quality relative to ductility and grain flow, it was apparent that an acceleration factor was operative in the several actual failures, and in as much as the surface was uncoated, with shot peening protection only, an environmental or corrosion factor was suspected. There were three mechanisms of interest involving an environmental factor: stress corrosion, hydrogen embrittlement, and low cycle corrosion fatigue. The available literature and experience were reviewed for information on these mechanisms applicable to low alloy steel heat treated to 260-280 ksi tensile strength. The results of this enlightened attempt were very discouraging. Basically it was apparent that very few of the required technical answers were available, even in this basic aircraft steel, to use in a logical analysis of fracture mechanism by deduction from experimental observations. Consultants were asked to assist in the analysis but their findings were equally discouraging.

By this time, the contractor had underway an extensive program involving accelerated stress corrosion tests, additional qualification tests, and various material quality tests (including a re-evaluation of forging design and material selection), but the results were not leading to isolation of the failure mechanism. For example, in stress corrosion tests, the bare shot peened specimens were outlasting all the various protective coating systems evaluated. Finally, the Directorate of Materials and Processes (ASD) suggested that the contractor use the only remaining possibility for clarification of the embrittling mechanism - one of the electron microscope fractography techniques in use in only two industrial facilities in the country. Fortunately, the facilities of both aircraft companies were made available, and the results from one of these organizations are shown in figure 30. The independent results of both organizations attributed the initial intergranular cracking to hydrogen embrittlement. This conclusion was not a simple one, because of the similarities between hydrogen embrittlement and stress corrosion failures in high strength low alloy steels; however, similar independent results would lend weight to the accuracy of the conclusion.

Assuming the failure is due to hydrogen embrittlement, we now have the interesting problem of finding the source of hydrogen, so that it might be eliminated. Plating or acid pickling was not permitted on the gear during or after processing and no protective coating was applied to the fillet area. At one time an X-38 coating, which consisted of a

phosphate pre-treatment plus a moly-disulfide coating which acts as a dry film lubricant, was applied to the fillet area. This was subsequently removed because of poor galling characteristics. The axle beams were baked 3 hours at 375°F after removal of the moly-disulfide coating. This should have removed the hydrogen present. As you can see, no obvious explanation can be given as to the origin of the hydrogen that caused the embrittlement failure.

One additional cracked axle was discovered during a jacking operation in January, 1962, where the original failures (in the highly stressed fillet area) were eliminated by removal of the integral axles and installation of separate "thru-axles" to carry the primary loads. (This modification increased over all gear weight by 100 percent and is a prohibitive weight penalty - a lighter weight more reliable design is being developed.) The cracked axle of the "thru-axle" design is shown in figure 31. The crack now occurred on the top side, in the forging parting line, but was not catastrophic as the cracking stopped when the low stress area was encountered. The modification has not eliminated the cracking but has served to prevent catastrophic failures by substitution of a moderate strength AISI 4340 axle (180-200 ksi UTS) as the critically loaded component. The fracture surface (figure 32) again shows an intergranular initiation zone. Note that over 50 percent of the fracture occurred by intergranular cracking and the axle assembly was still performing adequately under regular service conditions. The electron fractographs shown in figure 33 supposedly confirm the occurrence of hydrogen embrittlement.

The fractured truck beam of the main landing gear assembly shown in figure 34 is believed to be the first stress corrosion failure encountered in high strength low alloy steel axles (AISI 4340 heat treated to 260-280 ksi UTS). The failure occurred during a normal towing operation, September 1961. The general view of the assembly shows the through-axle design with the axle retaining bolt on each side; the gear is coated with an epoxy paint to protect against corrosion. A close-up of the fracture origin (figure 35) shows the cracking originated in the forward inboard bolt hole.

Approaching the origin at higher magnifications, the origin is seen as a discolored semi-circle with faint concentric rings (not clearly evident in photographs). The discolored origin was approximately 0.03 by 0.05 inches and the largest concentric ring measured 0.40 inches; the entire origin exhibited "brittle" intergranular cracking which shows in the photomicrograph and electron microscope fractograph shown in figure 36.

The material quality was checked and found to be excellent, as indicated by the longitudinal tensile properties (percent reduction in area exceeding 30 percent and notched/unnotched strength ratio exceeding one). Examination of the fracture surface eliminated fatigue as the cracking mechanism, and hydrogen embrittlement seemed unlikely because of the lack of hydrogen-inducing conditions during processing. However, the conclusion that stress corrosion cracking was responsible was finally reached based primarily on the appearance of the electron microscope fracture-surface replicas, and the differences in appearance between hydrogen and stress corrosion failure.

Analysis of this September 1961 failure during towing again serves to emphasize the difficulties in pinpointing the cause of failures in high strength steels and points out the usefulness of the electron microscope fractographic analysis techniques. Although this analysis is believed to be accurate, it is obvious that additional research effort is needed unequivocally to establish the distinctions between the fracture appearances to eliminate confusion especially since these techniques are being adopted by more and more organizations throughout the country.

CONCLUSION

The characteristic appearance of fatigue fractures (at least low stress-high cycle fatigue cracks) permits straightforward identification, due to the arcs or "breach marks" on the fracture surface, and a transgranular cracking mode. Identification of stress corrosion cracking in aluminum alloys is also reasonably simple due to the shiny, intergranular cracking zone at the failure origin; frequently evidence of secondary cracking can also be found. Identification of stress alloying cracking is usually facilitated by the process of globules of the penetrating metal on the fracture surface and an intergranular cracking mode.

The big weakness in effective service failure analysis involves the lack of knowledge regarding the fracture surface appearances of hydrogen embrittlement, stress corrosion, corrosion fatigue and low cycle-high stress fatigue in high strength steel alloys. Because of the pronounced susceptibility of high strength steels to cracking mechanisms, it appears most urgent that the fractographic characteristics of these failure mechanisms must be developed as soon as possible.

Use of the electron microscope for high magnification examination of replicas from fracture surfaces apparently offers a capability for the resolution of the subtle differences in fracture appearances in high strength alloys. Measurement of the individual striations of highly magnified fatigue cracked surfaces may allow direct experimental measurement of the stress history of the fracture and allow an independent check on the accuracy of theoretical stress analysis procedures used by designers.

REFERENCES

(1) P. J. E. Forsyth, D. A. Ryder, A. C. Smale and R. N. Wilson, "Some Further Results Obtained from the Microscopic Examination of Fatigue, Tensile and Stress Corrosion Fracture Surfaces," Tech Note No. MET 312, Royal Aircraft Establishment (Farnborough), August 1959. ASTIA AD No. 230906.

(2) D. O. Sprowls and R. H. Brown, "What Every Engineer Should Know About Stress Corrosion of Aluminum," Metal Progress, Vol 81, No. 4 and 5, April and May 1962.

(3) D. O. Sprowls and R. H. Brown, "Resistance of Wrought High Strength Aluminum Alloys to Stress Corrosion," Alcoa Report, 20 June 1961.

(4) Armour Research Foundation, Effort on ASD Contract AF 33(616)-7612.

(5) E. A. Steigerwald, "Delayed Failure of High Strength Steel in Aqueous Environments," Proc ASTM 60 (1960) p 750.

(6) "Stress Corrosion Testing of High Strength Steels," Boeing Transport Division Quarterly Progress Reports, D6-7502, D6-7502-1, D6-7502-2, D6-7502-3, Contract AF 33(616)-7839.

(7) Col. E. M. Kennedy, Jr., "The Effect of Cadmium Plating on Aircraft Steels Under Stress Concentration at Elevated Temperatures," WADD-TR-60-486, September 1961.

(8) J. G. Morlet, H. H. Johnson and A. R. Troiano, "A New Concept of Hydrogen Embrittlement in Steel," WADC Technical Report 57-190 (ASTIA No. AD-118155), March 1957.

(9) H. H. Johnson, J. G. Morlet and A. R. Troiano, "Hydrogen, Crack Initiation and Delayed Failure in Steels," WADC Technical Report 57-262 (ASTIA No AD 118252), May 1957.

(10) P. A. Blanchard and A. R. Troiano, "Hydrogen Embrittlement in Terms of Modern Theory of Fracture," WADC Technical Report 59-444, August 1959.

(11) M. L. Hill, "The Behavior of Hydrogen Iron and Steel," American Electroplaters Society, Technical Proceedings, 1960, p 124.

(12) D. A. Bolstad and W. E. Quist, Boeing Document D6-7016, December 1960 (to appear in Metal Progress).

(13) K. E. McIntosh and N. B. Green, "Procedure For Determining the Hydrogen Embrittlement Susceptibility of 4340 Steel," North American Aviation, Inc. (Columbus Division).

(14) P. Lillys and A. E. Nehrenberg, "Effect of Tempering Temperatures on Stress-Corrosion Cracking and Hydrogen Embrittlement of Martensitic Stainless Steels," ASM Transactions, 68, 1956, p 327.

(15) R. A. Davis, "Stress Corrosion Investigation of Two Low Alloy High Strength Steels," presented at the 18th NACE Conference in Kansas City, March 19-23, 1962.

TABLE I

INCREASE IN STRENGTH REQUIREMENTS FOR ENGINEERING METALS

ALLOY SYSTEM	YIELD STRENGTH (KSI) YEARS				
	1945	1950	1955	1960	1965
STEEL	150	165	180	225	275
TITANIUM	60	100	150	175	200
ALUMINUM	70	70	70	75	80
MAGNESIUM	25	30	35	45	60

SERVICE FAILURE ANALYSIS INVOLVING BRITTLE CRACKING MECHANISMS

TABLE 2

DELAYED FRACTURE CHARACTERISTICS

INFLUENCE OF VARIOUS ENVIRONMENTS

STRENGTH YS/UTS(ksi)	ENVIRONMEMT	APPLIED STRESS (ksi)	FAILURE TIME (min)
168/187	NTS	155	—
	DISTILLED WATER	140	600 (EST.)
		120	10,000
205/226	NTS	140	
	DISTILLED WATER	140	1
		130	10
		93	100
		40	1,000
		25	10,000
245/295	NTS	90	—
	DISTILLED WATER	75	6.5
	BUTYL ACETATE	75	18.0
	BUTYL ALCOHOL	75	28.0
	ACETONE	75	120
	LUBRICATING OIL	75	150
	RECORDING INK	75	0.5

300 (Cr-Ni-Mo low alloy steel)

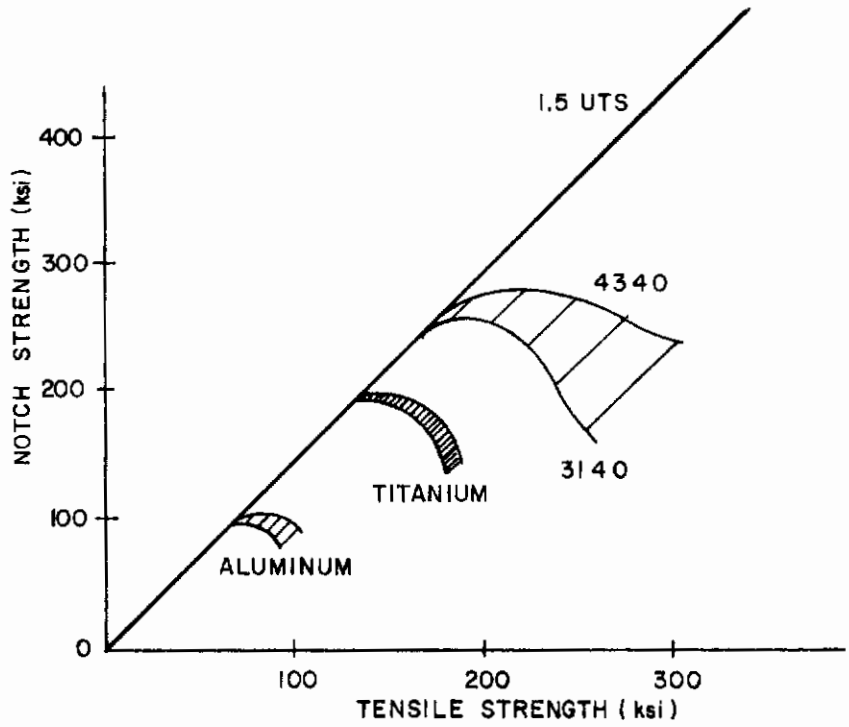

Figure 1. Notch Sensitivity vs Tensile Strength

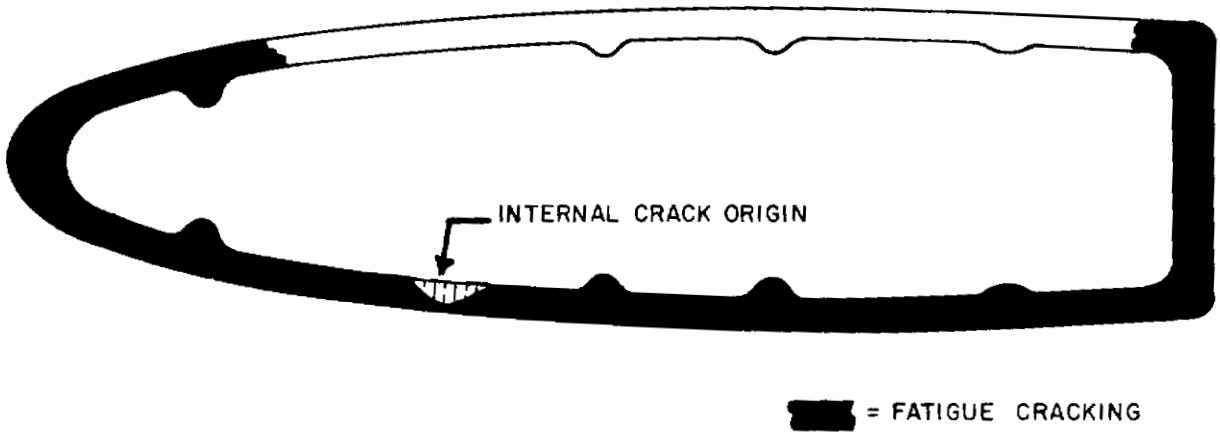

Figure 2. Fatigue Damage Helicopter Main Rotor Blade

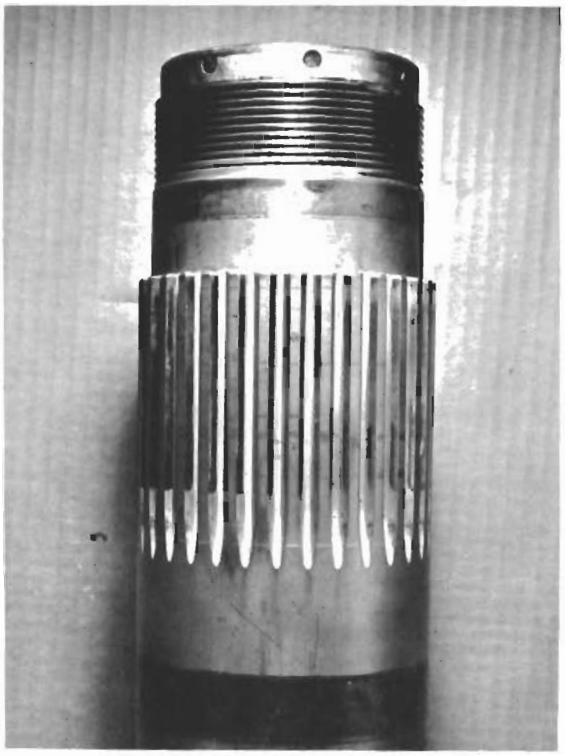

(a) Cracked Gear Shaft

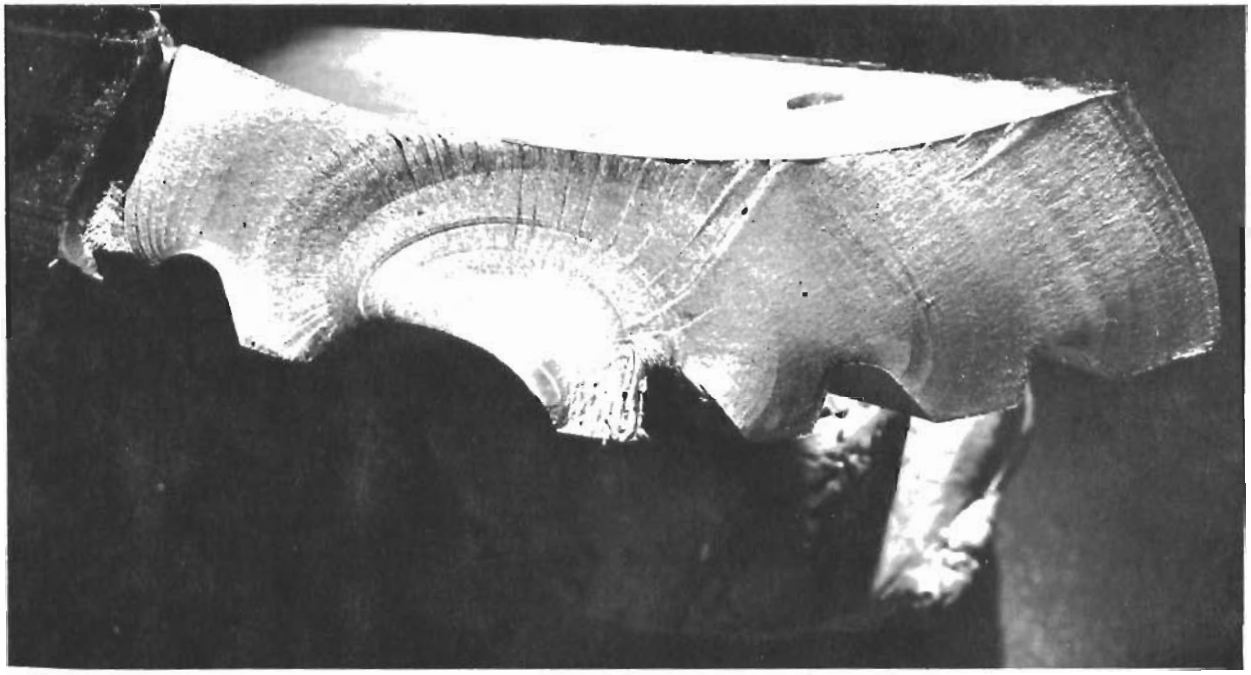

(b) Concentric "sea shell" Pattern of Fracture Surface

Figure 3. Fatigue Cracking in Propeller Gear Shaft of Large Transport Aircraft (AISI 4340 heat treated to 150-180 ksi UTS)

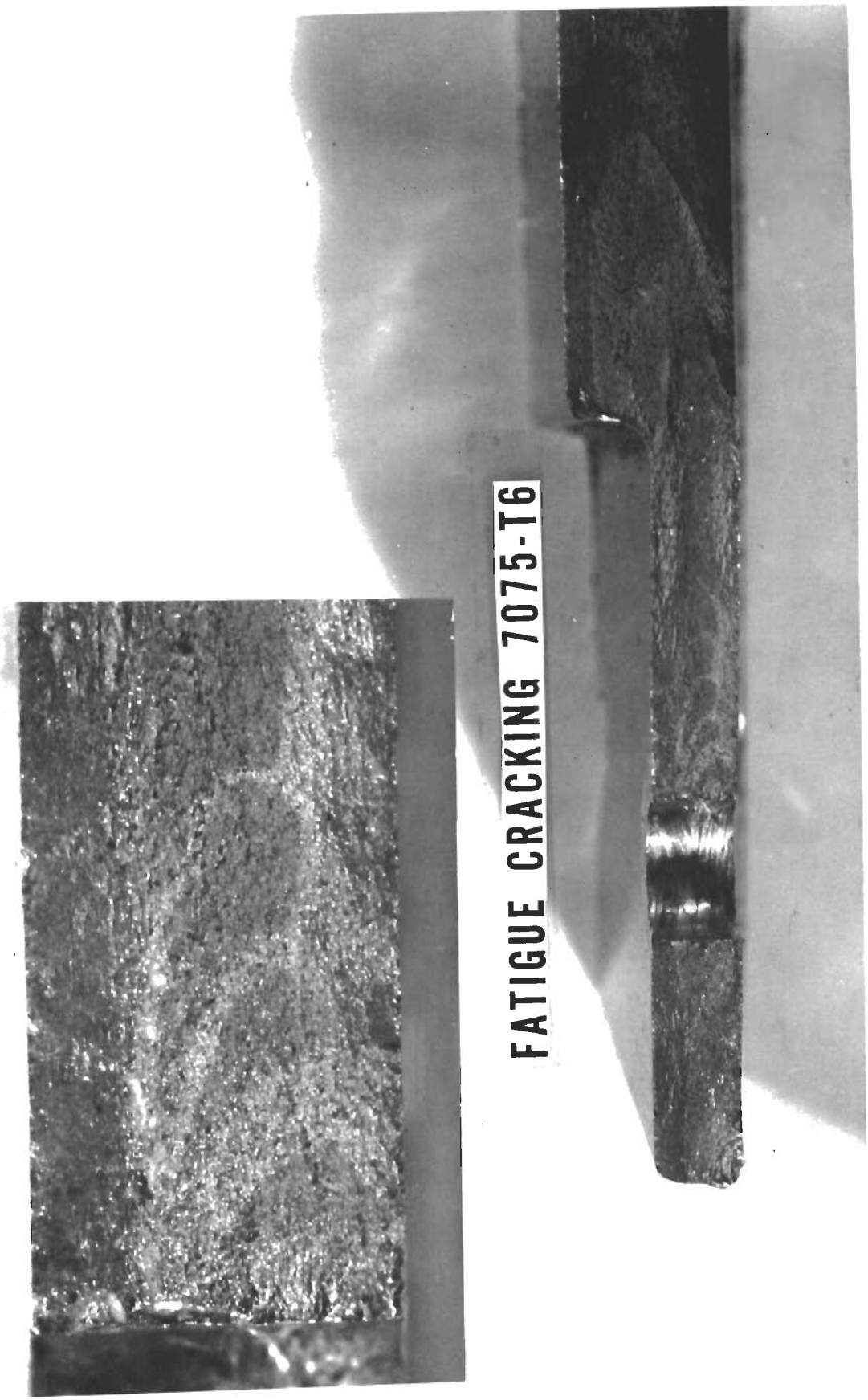

Figure 4. Low Cycle-High Stress Fatigue

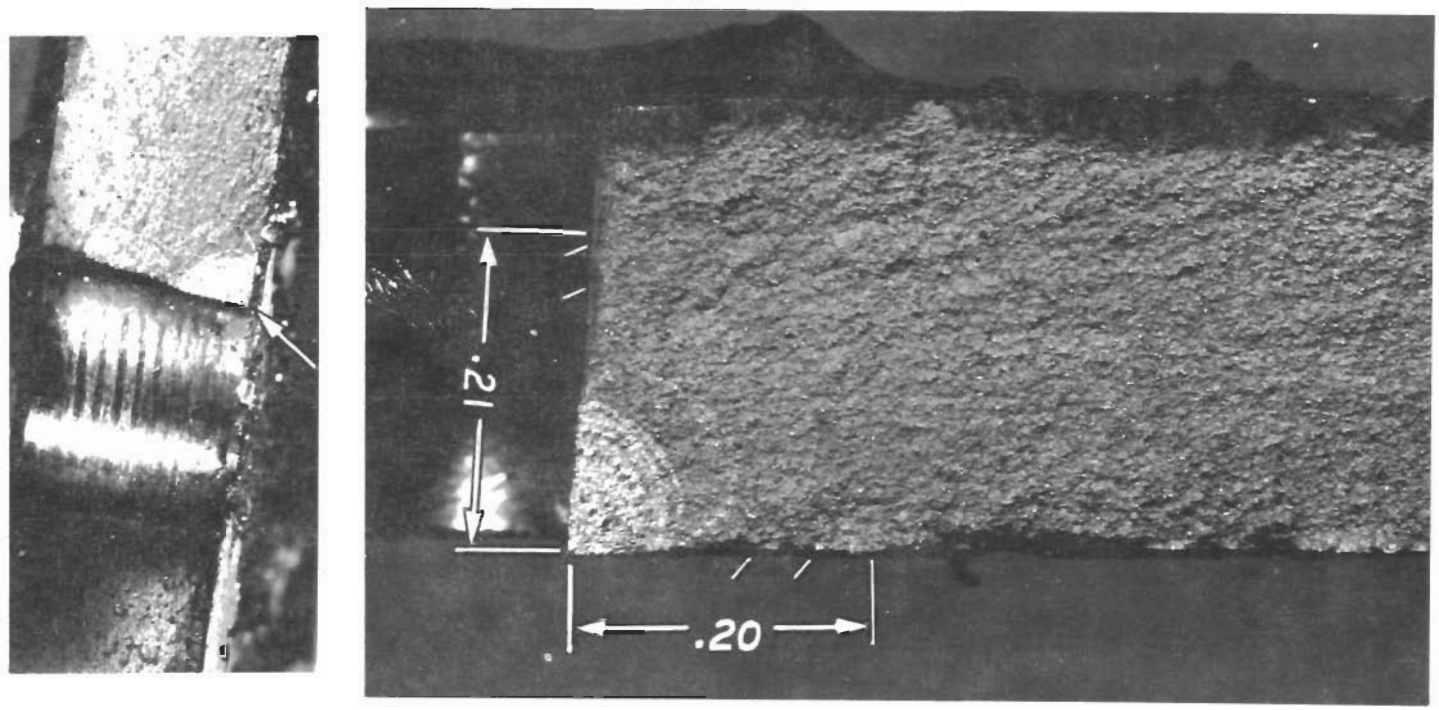

Figure 5. Catastrophic Failure Integral Wing Skin Panel Low Cycle-High Stress Fatigue

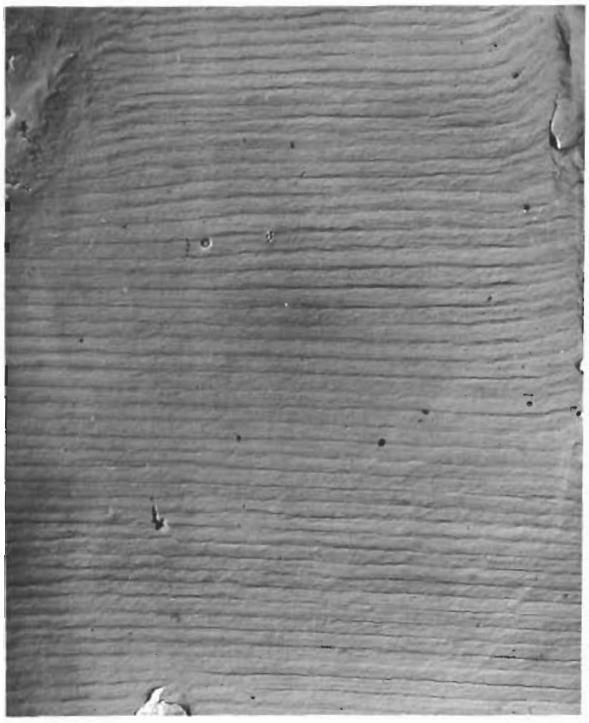

(b) Rene' 41 Alloy

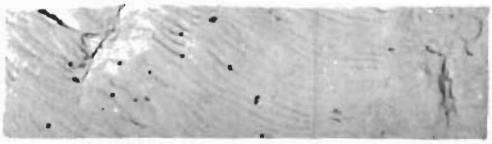

(d) Tantalum

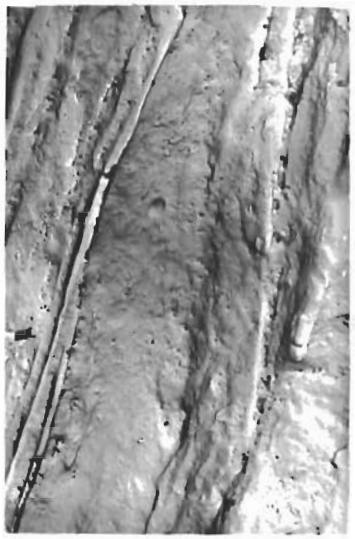

(c) Molybdenum

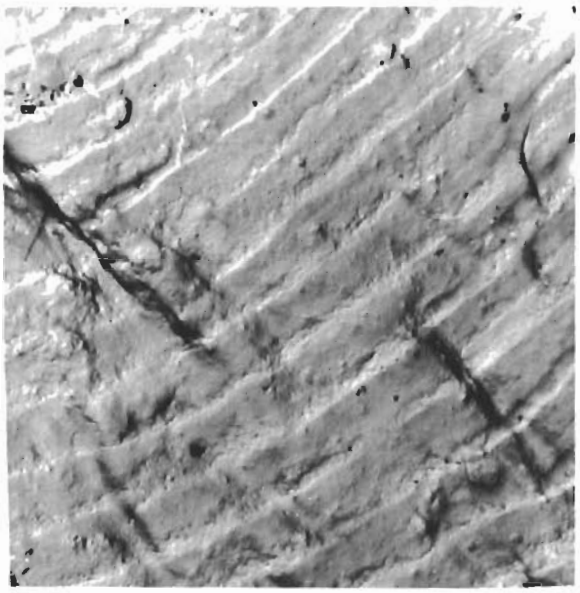

(a) 2024 Aluminum Alloy

Figure 6. Electron Microscope Replica Photographs of Fatigue Fracture Surface

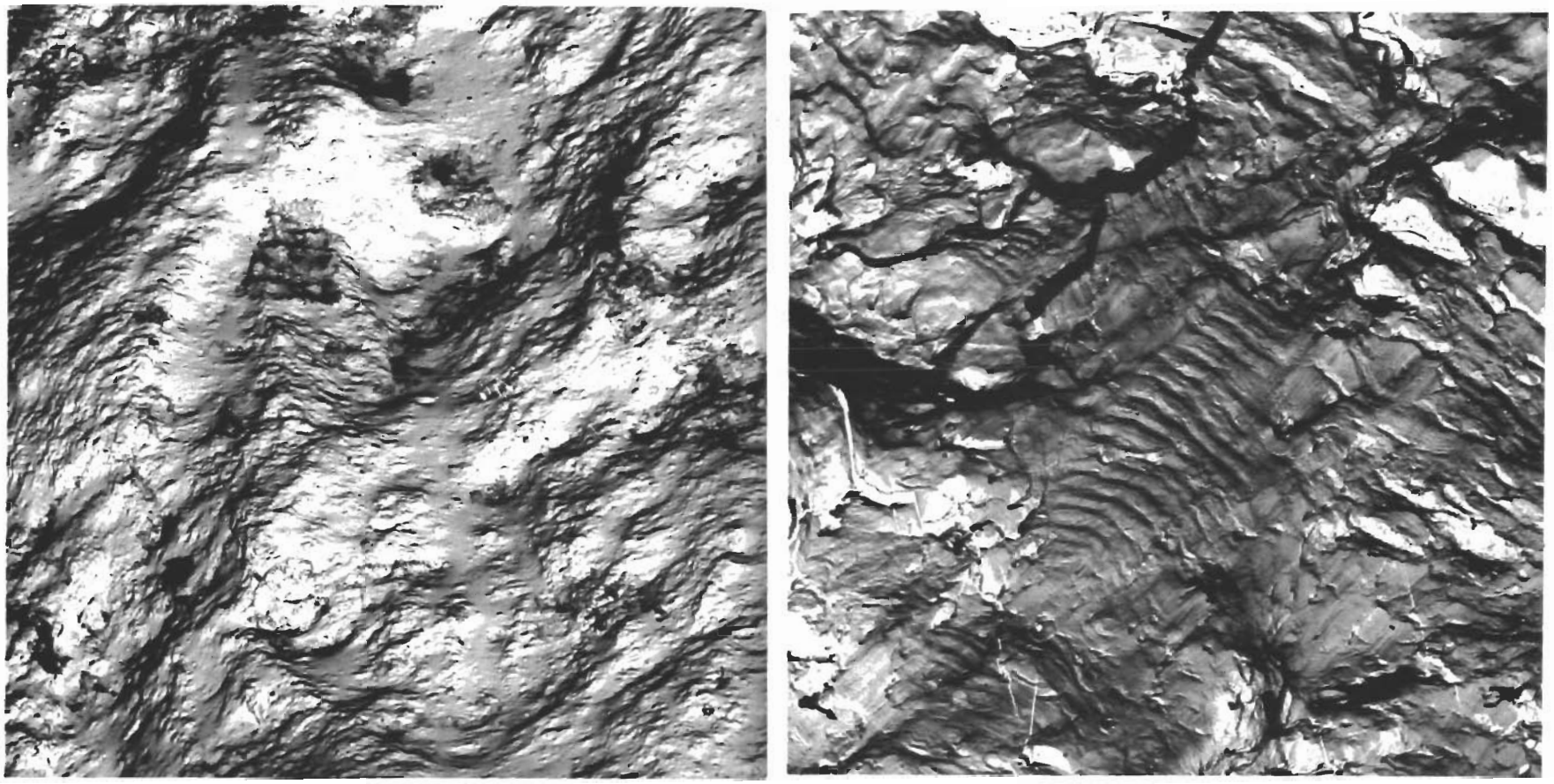

(a) Low Cycle Fatigue (AISI 4340; 260-280 ksi UTS)
130 ksi, 32000 Cycles to Failure

(b) High Cycle Fatigue (AISI 4330 M; 220-240 ksi UTS)
80 ksi, 994000 Cycles to Failure

Figure 7. Fractographs of Fatigue Cracked Surfaces

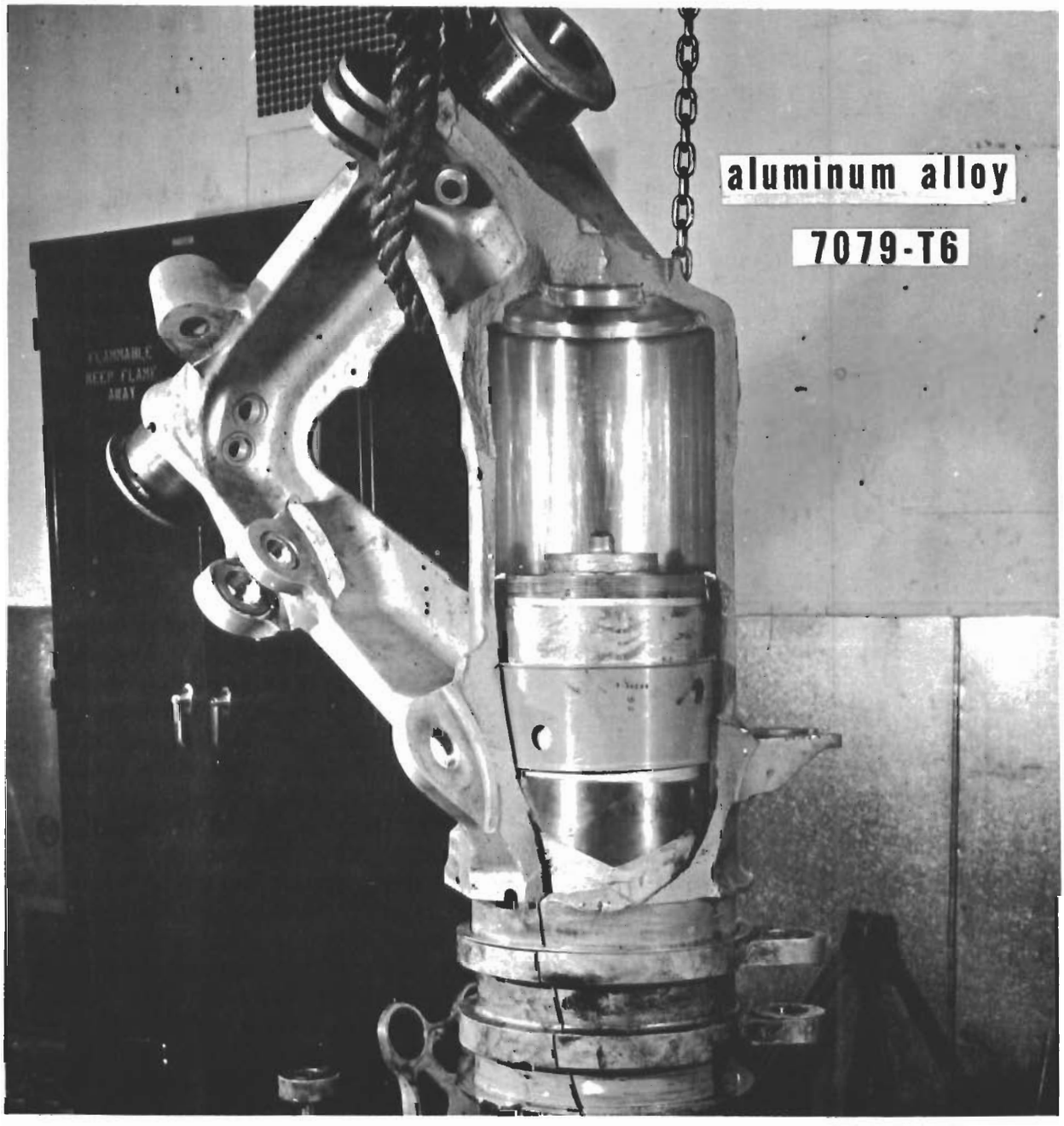

Figure 8. Stress Corrosion Cracking Landing Gear Cylinder

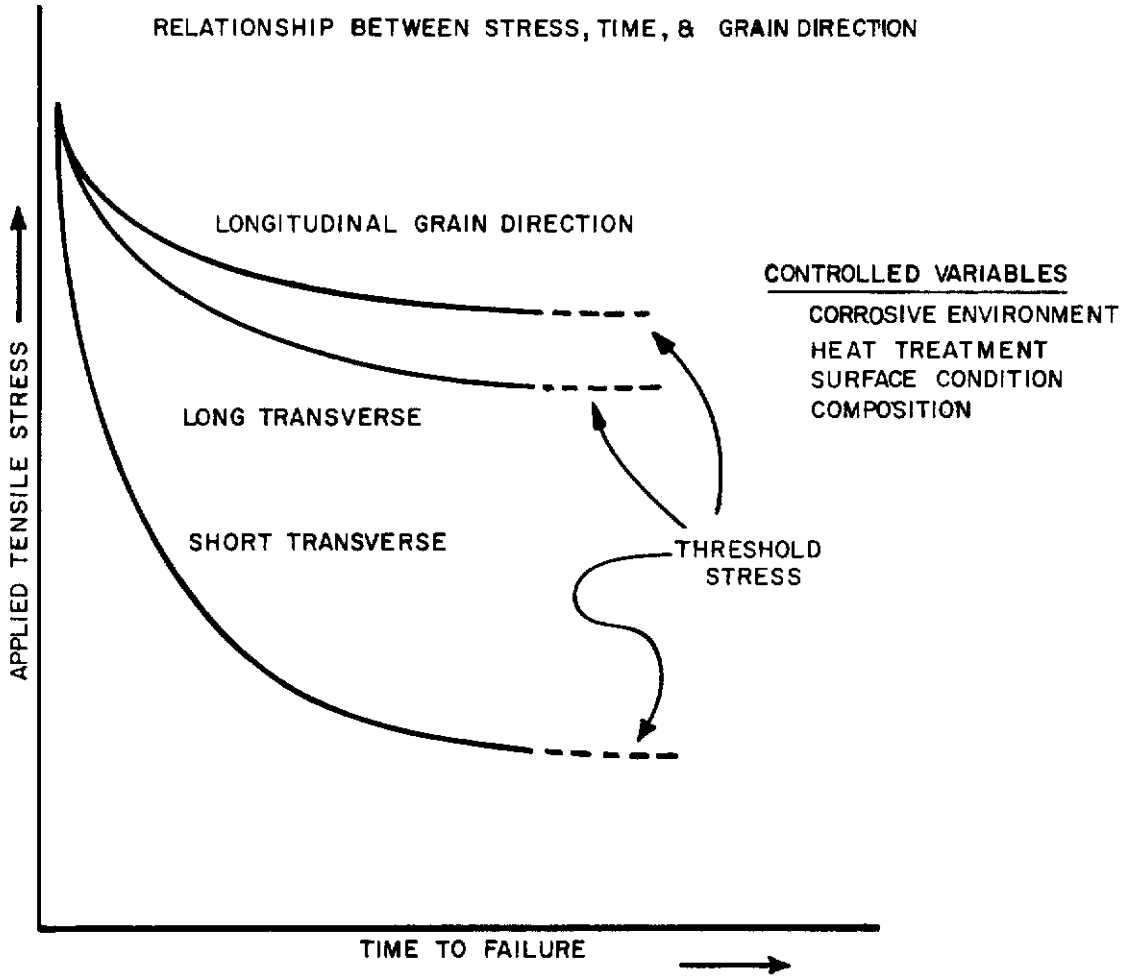

Figure 9. Stress Corrosion Cracking Susceptibility

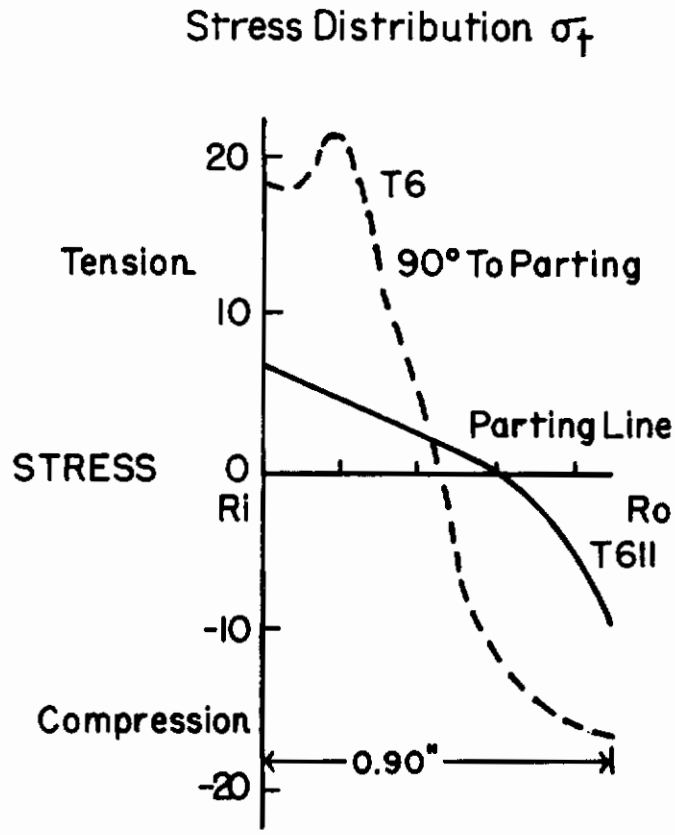

Figure 10. Residual Stresses in a Landing Gear Cylinder Showing Comparison of T6 (Coldwater Quench) and T611 (Hot Water Quench) Heat Treatments

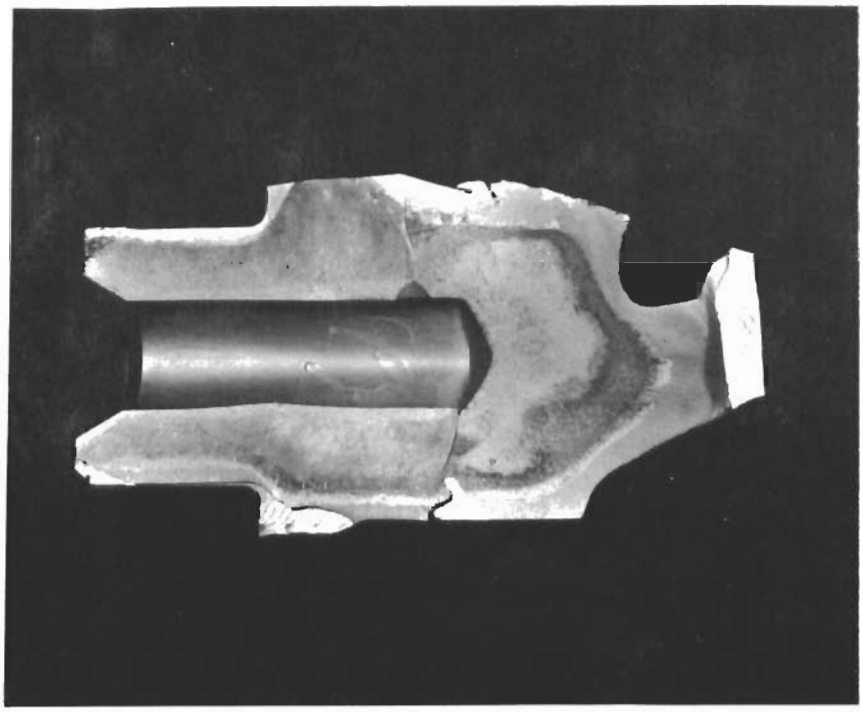

STRESS CORROSION CRACKING MAIN LANDING GEAR 7079-T6

FACTURE APPEARANCE

GRAIN FLOW PATTERN

Figure 11. Top Steeple Cracking

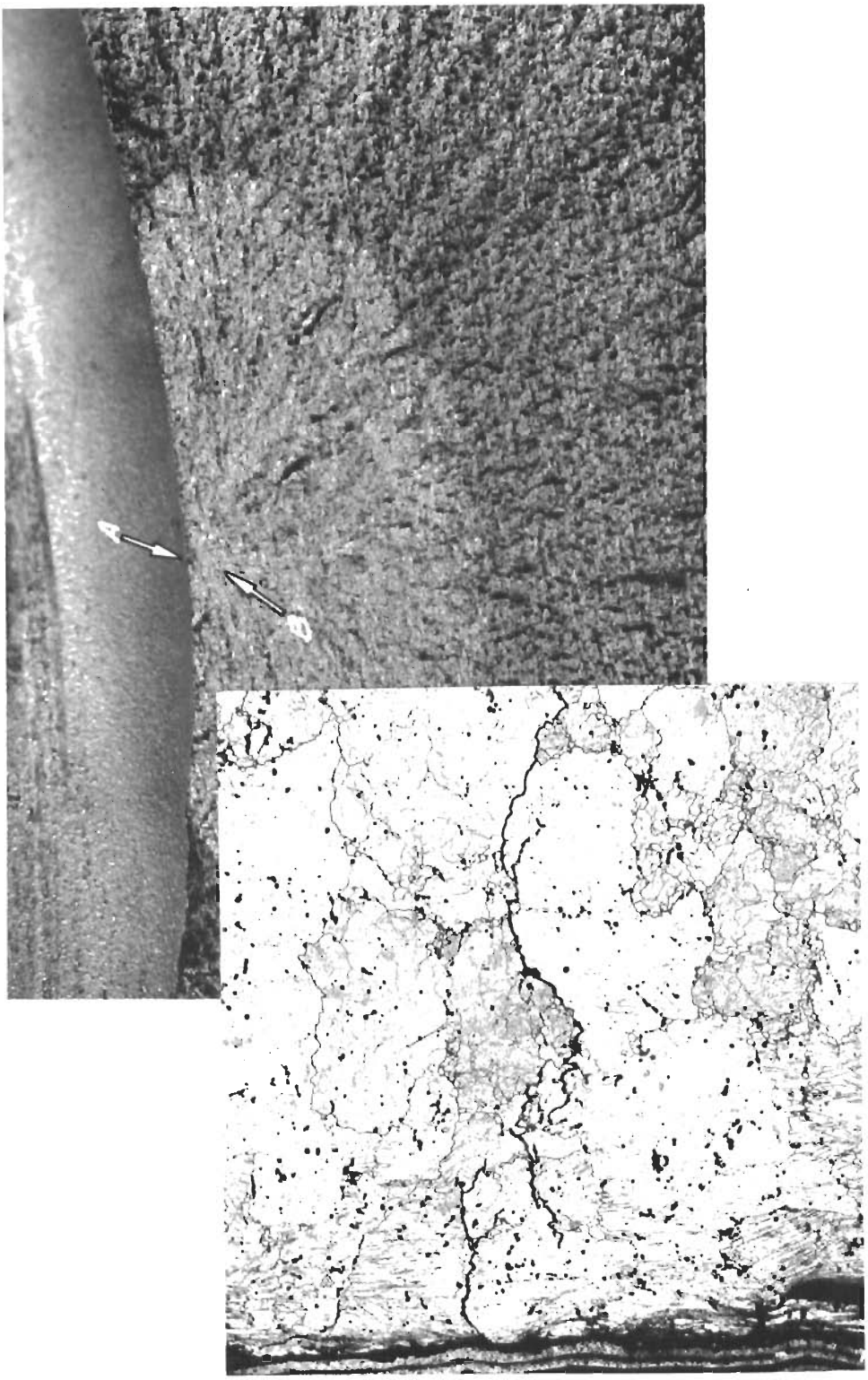

Figure 13. Fracture Face - Stress Corrosion Cracking Aluminum Alloys (7079-T6)

Figure 12. Intergranular Stress Corrosion Cracking - Aluminum Alloys (7079-T6)

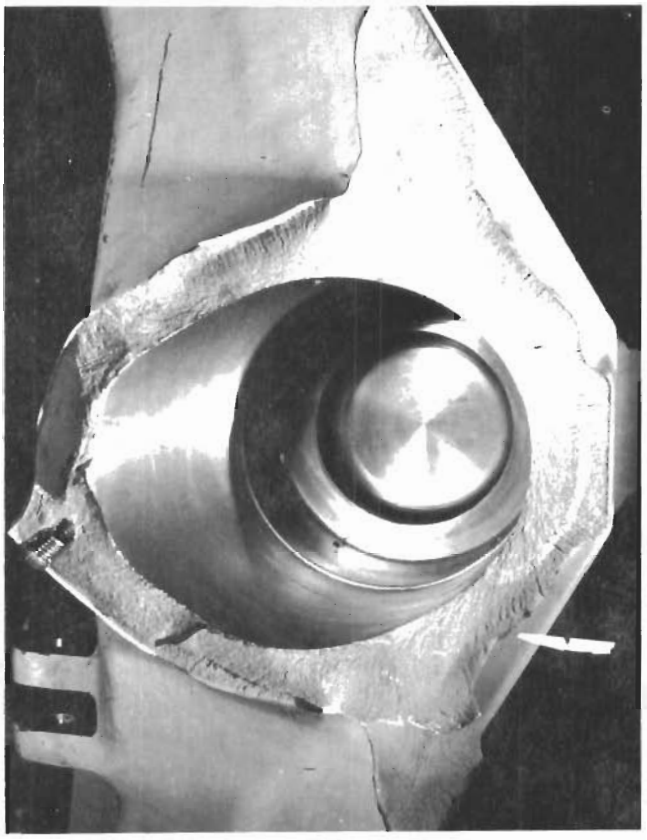

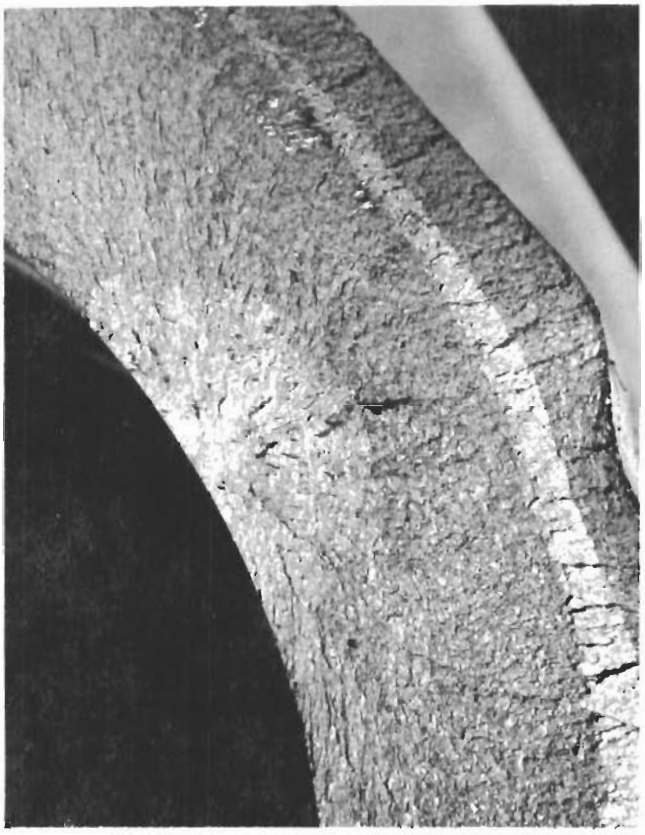

MULTIPLE CRACKING STAGES 7075 - T6

Figure 14. Stress Corrosion Cracking - Main Landing Gear

Figure 15. Interaction of Surface Pits With Stress Corrosion Cracking Mechanism (7079-T6 Aluminum Alloy)

Fracture Surface Replica -
Electron Microscope

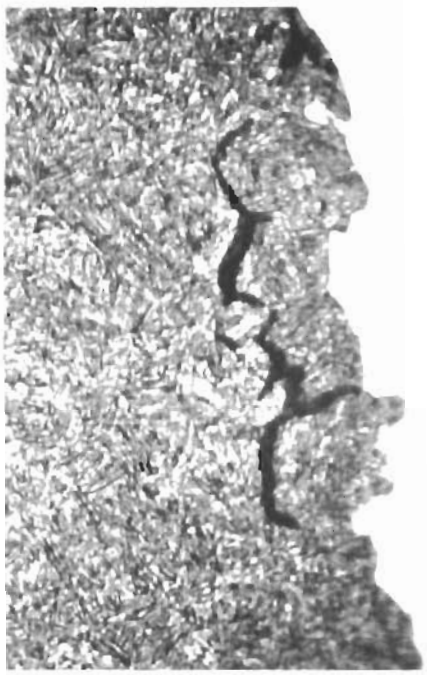

Optical Metallography
Cross Section

Figure 16. Stress Corrosion Fracture of Landing Gear Axle (AISI 4340 Heat Treated to 260-280 ksi UTS)

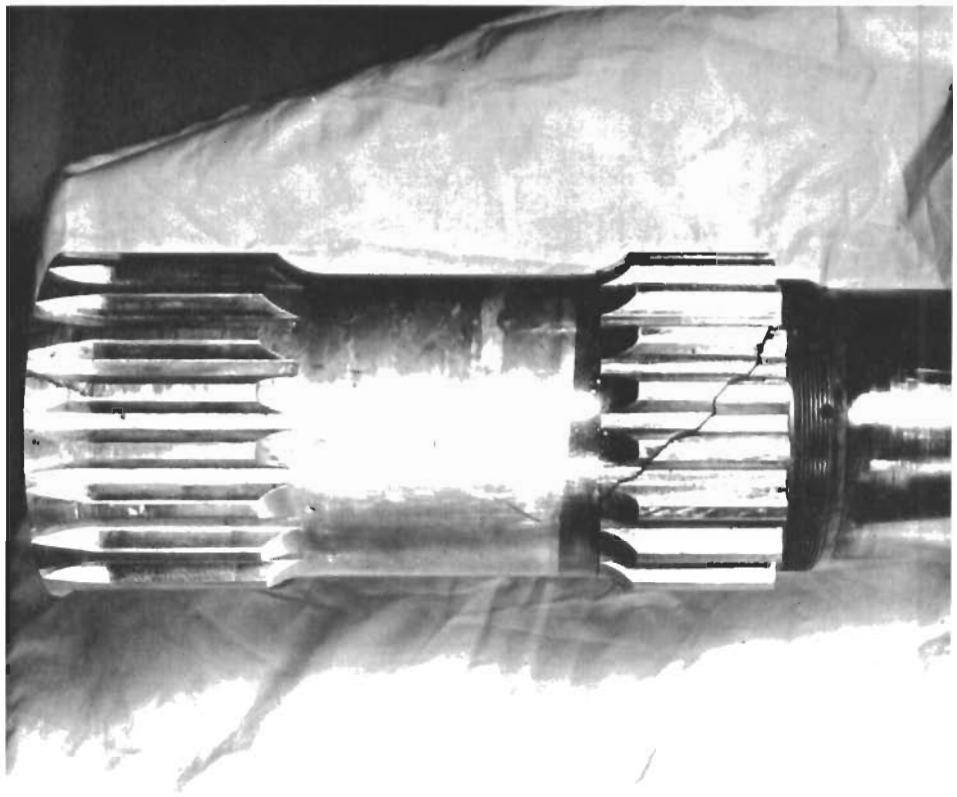

(b) Crack-Main Gear Axle

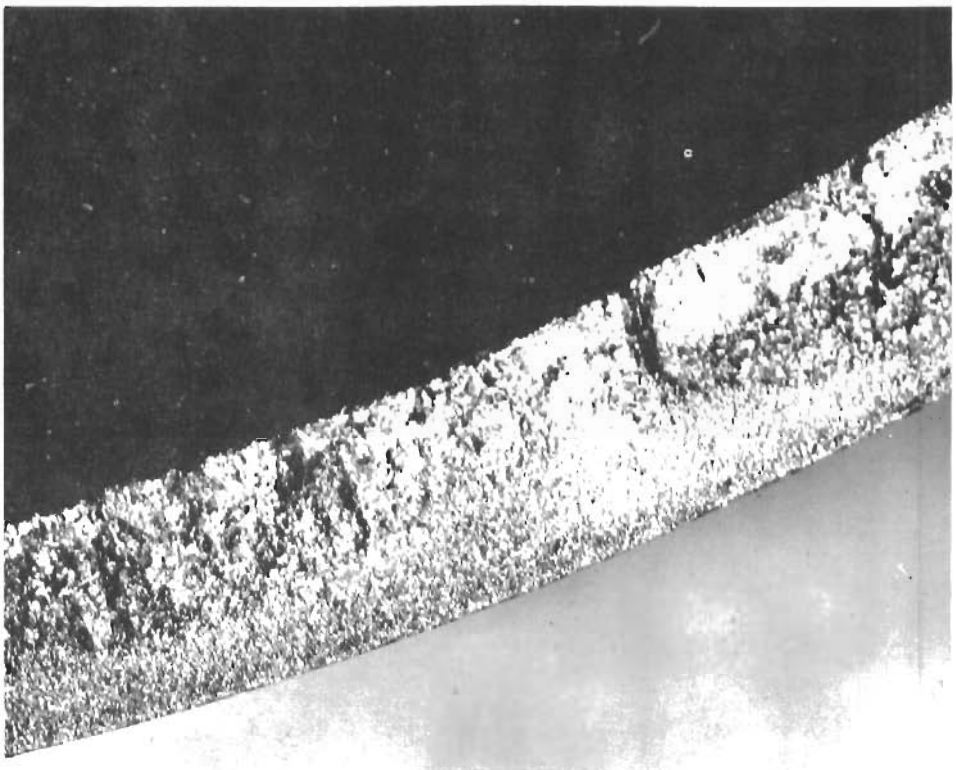

(a) Axle Fracture Face

Figure 17. Stress Alloying Behavior of Cadmium Plated Steel HY-TUF (220-240 UTS)

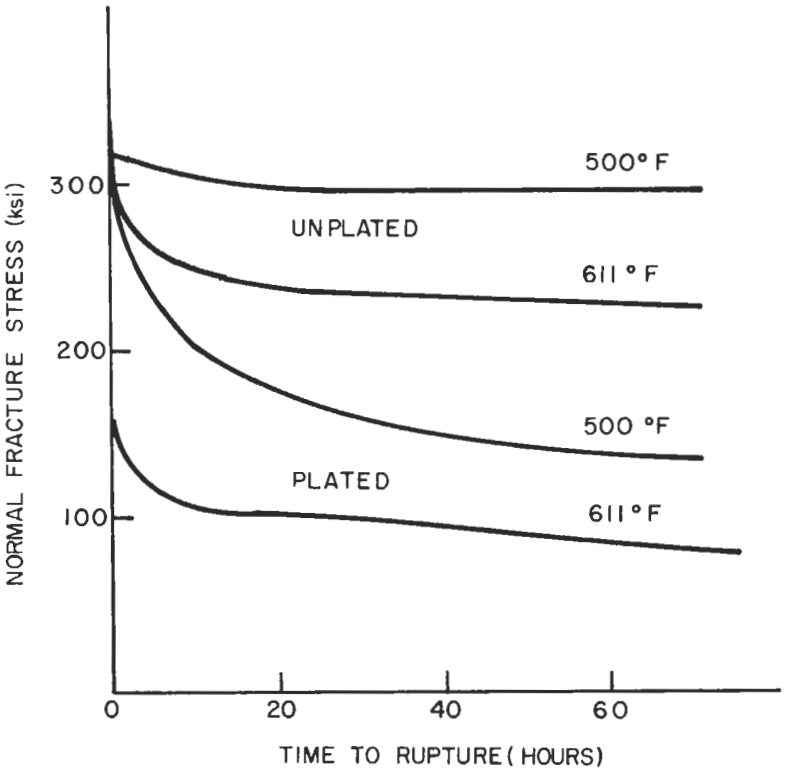

Figure 18. Stress Alloying Behavior of Cadmium Plated Steel AISI 4340 (240 ksi UTS)

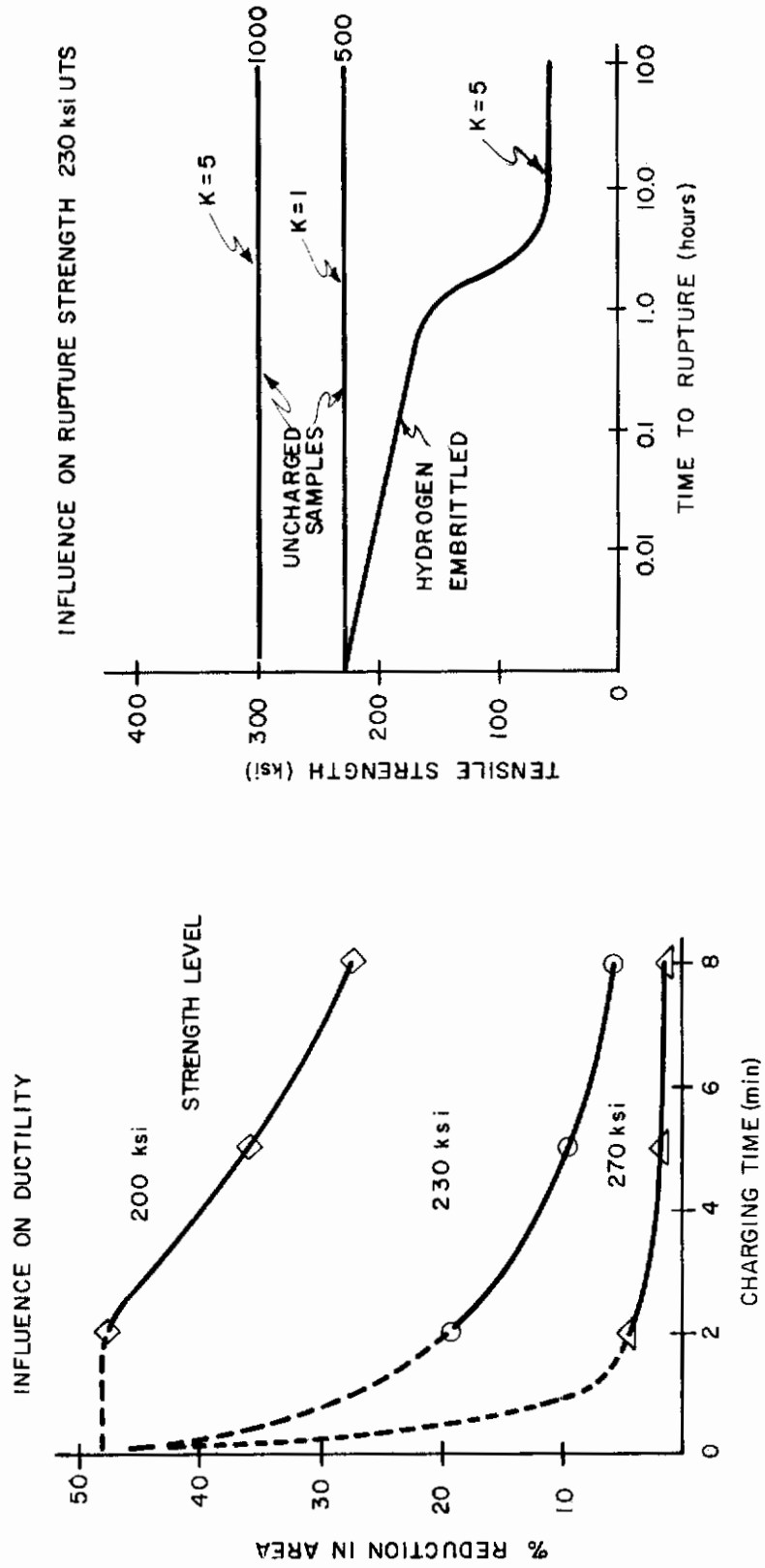

Figure 19. Effect of Hydrogen on AISI 4340

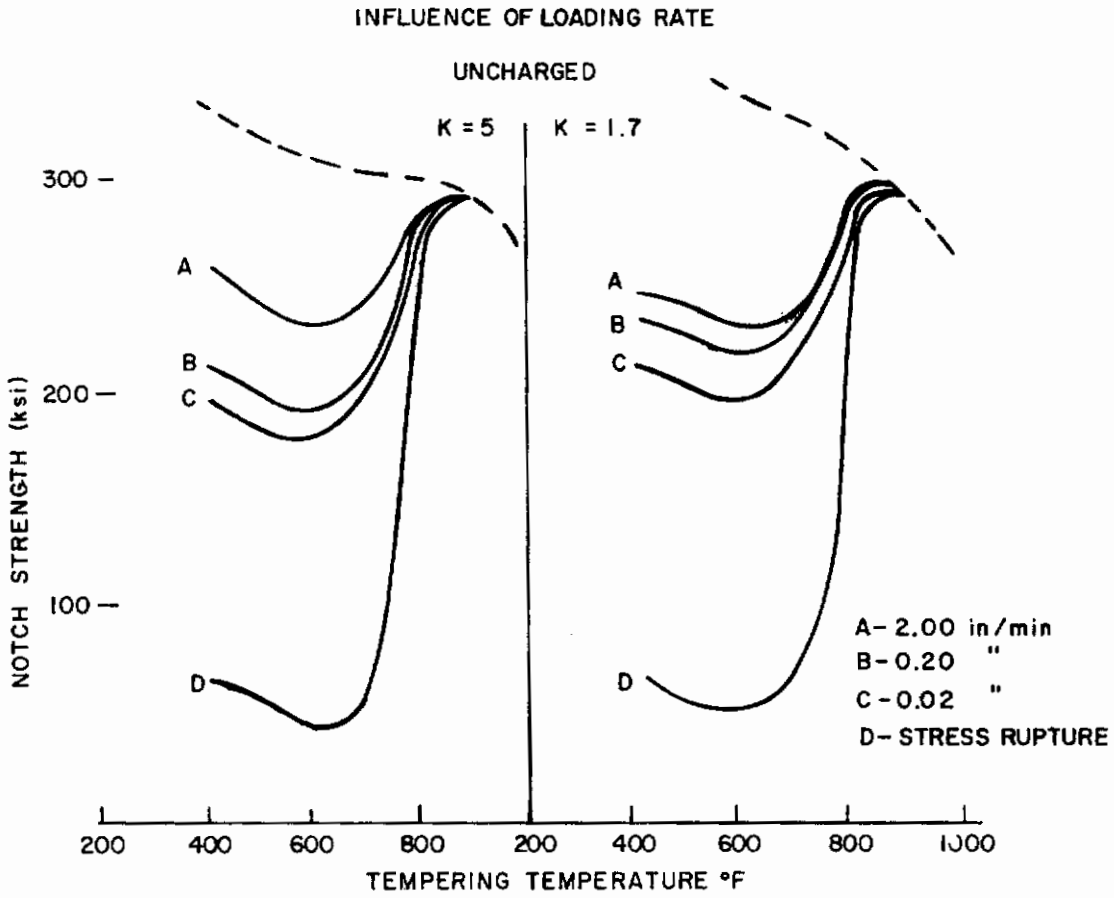

Figure 20. Effect of Hydrogen Embrittlement AISI 4340

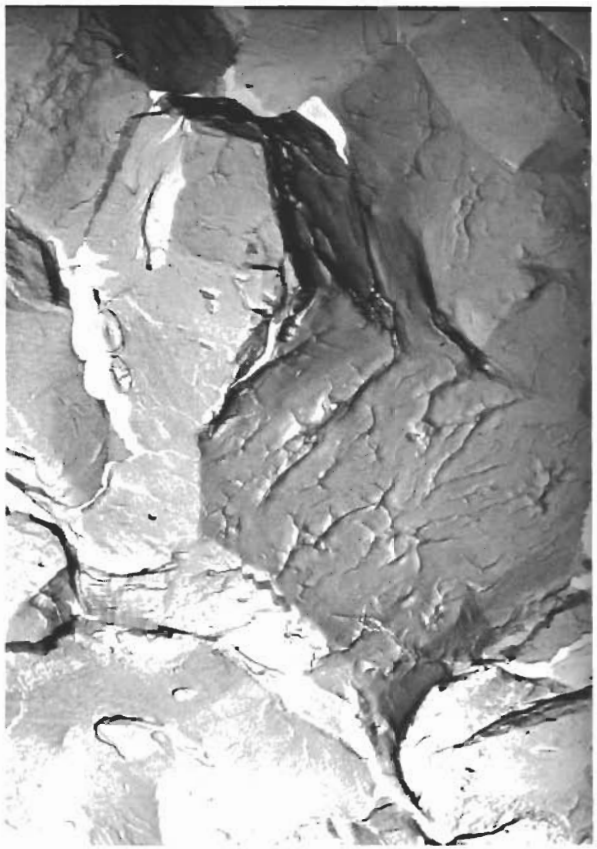

(a) Stress Corrosion Fracture
AISI 4340 (260-280 ksi UTS)
3.5% NaCl 11500 x

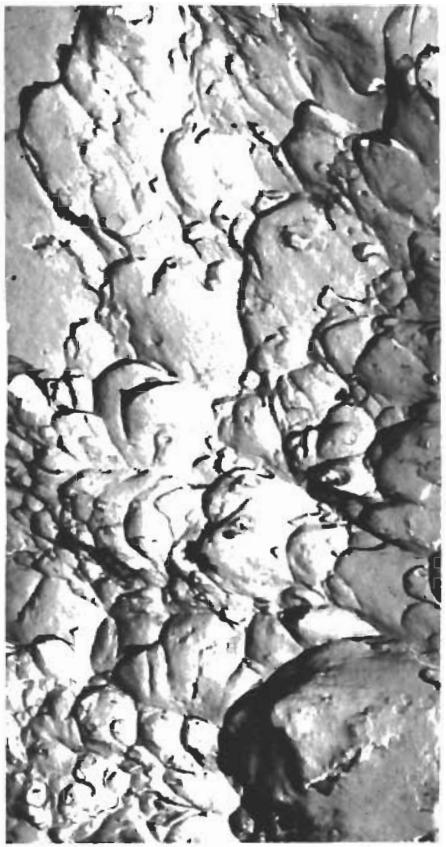

(b) Ductile Fracture 1300 x

(c) Hydrogen Embrittlement Fracture
AISI 4340 M (220-240 ksi UTS)
7000 x

Figure 21. Fracture Appearance of Low Alloy Steel (Electron Microscope Replication)

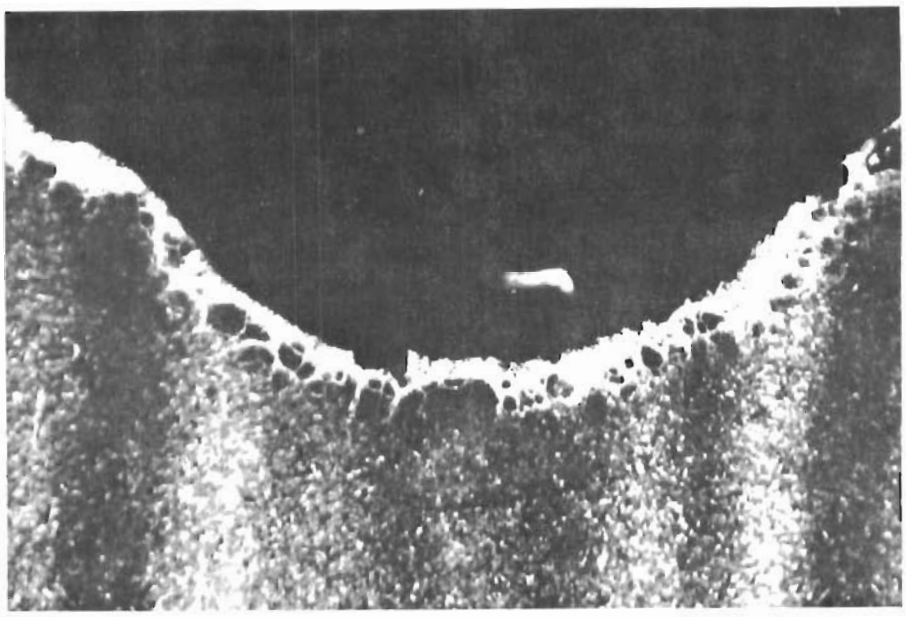

ALKALINE CHROMATE ETCH 500X AISI 4340

Figure 22. Intergranular Oxidation and Banding

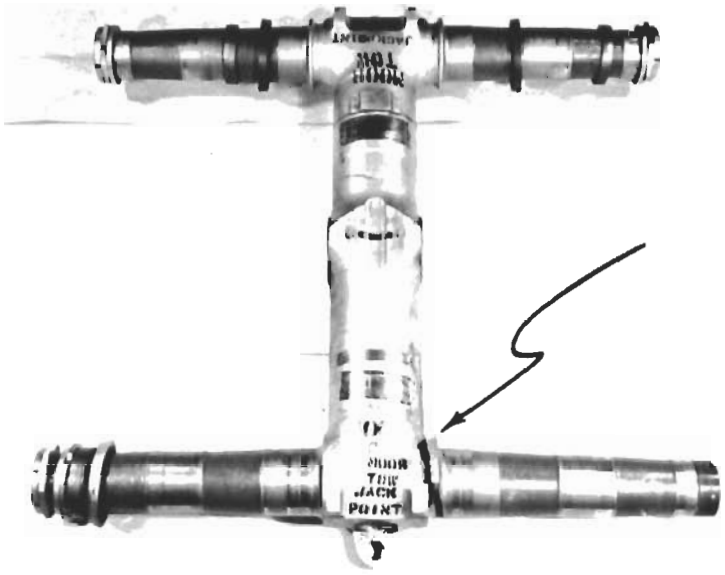

(a) View of Fractured Axle Beam 7/61 AISI 4340 (260-280 ksi UTS)

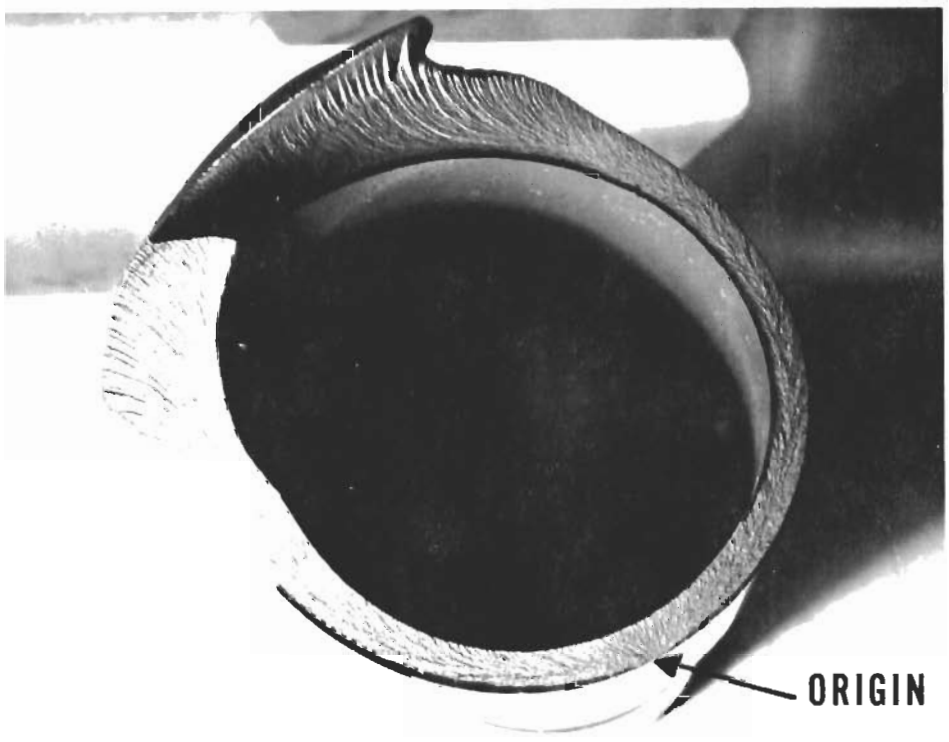

(b) Fracture Origin (Lower Radius) of Axle Beam 7/61

Figure 23. Axle Beam Failure

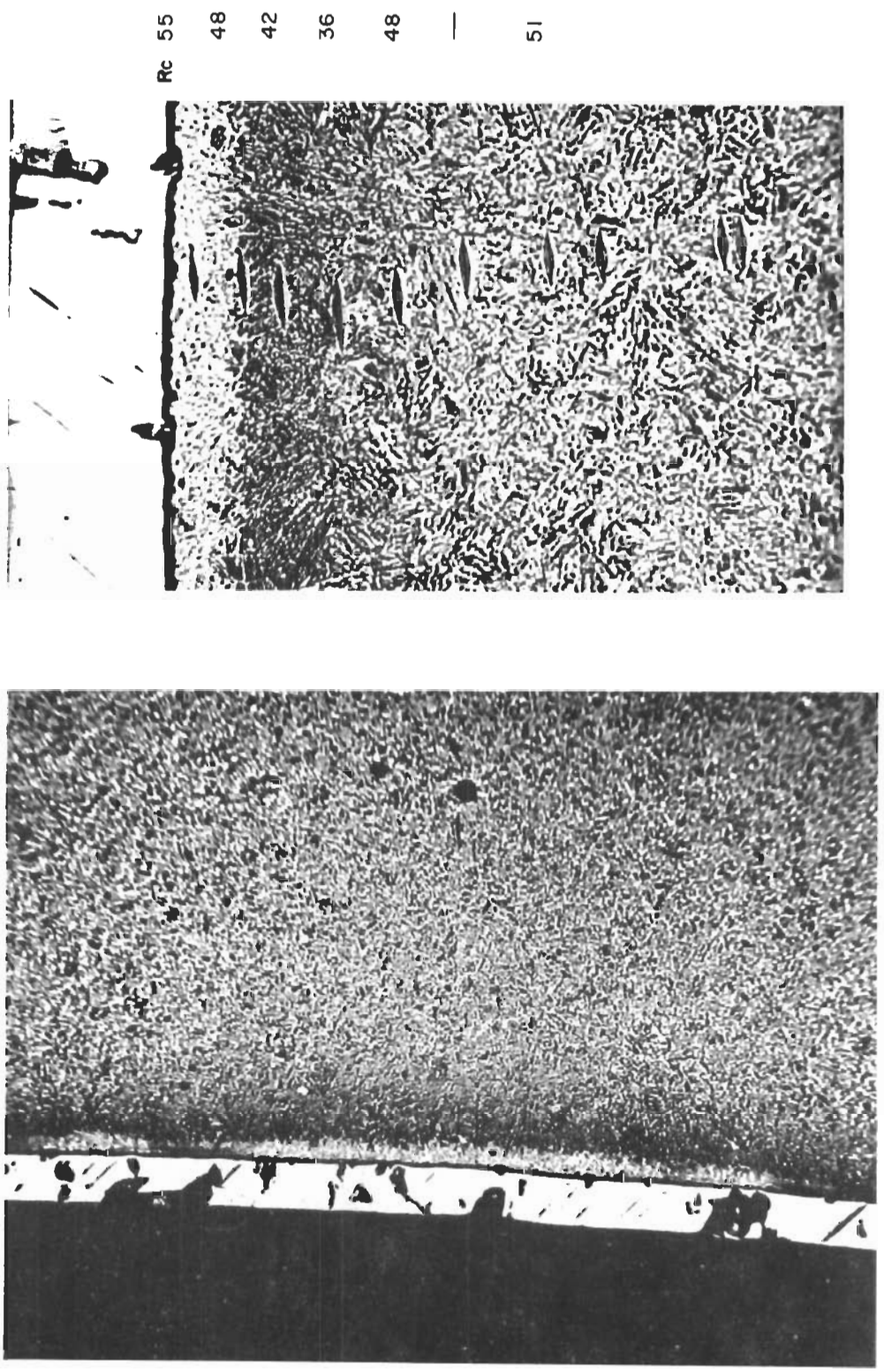

Figure 24. Surface Grinding Burns - Axle Beam Failure 7/61

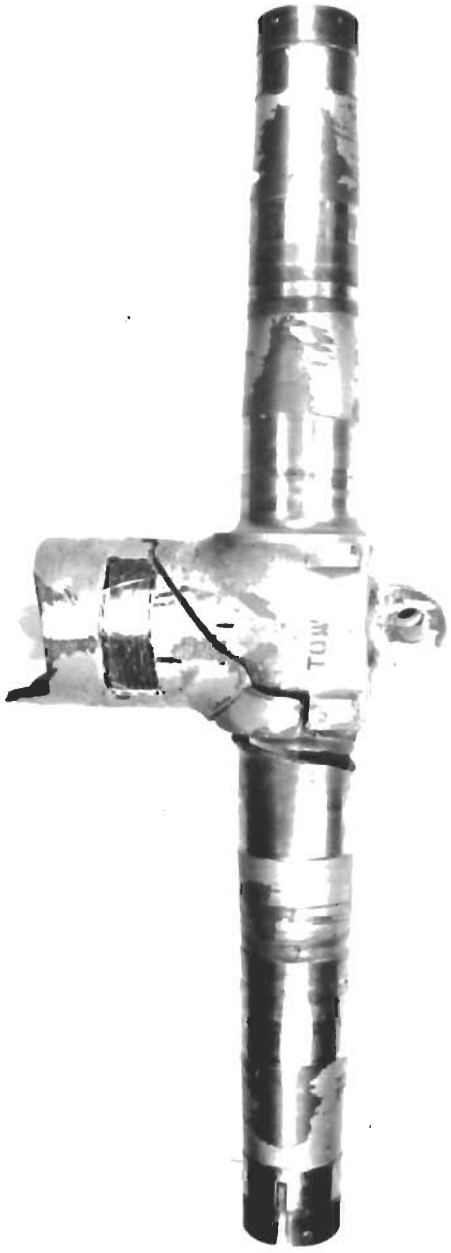

Figure 25. View of Fractured Axle Beam 9/61 AISI 4340 (260-280 ksi UTS)

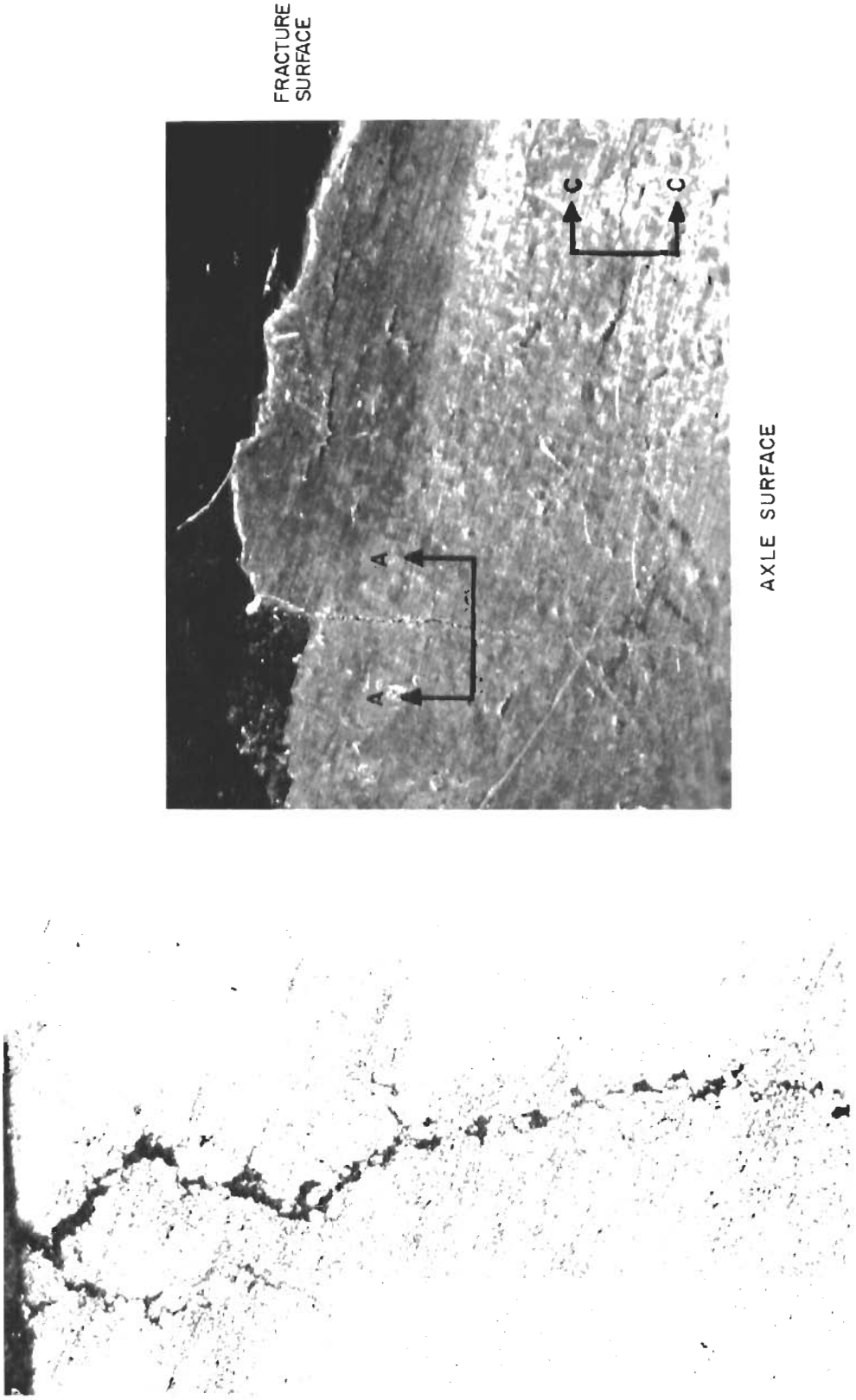

Figure 26. Intergranular Cracking Near Fracture Origin Axle Beam Failure 9/61

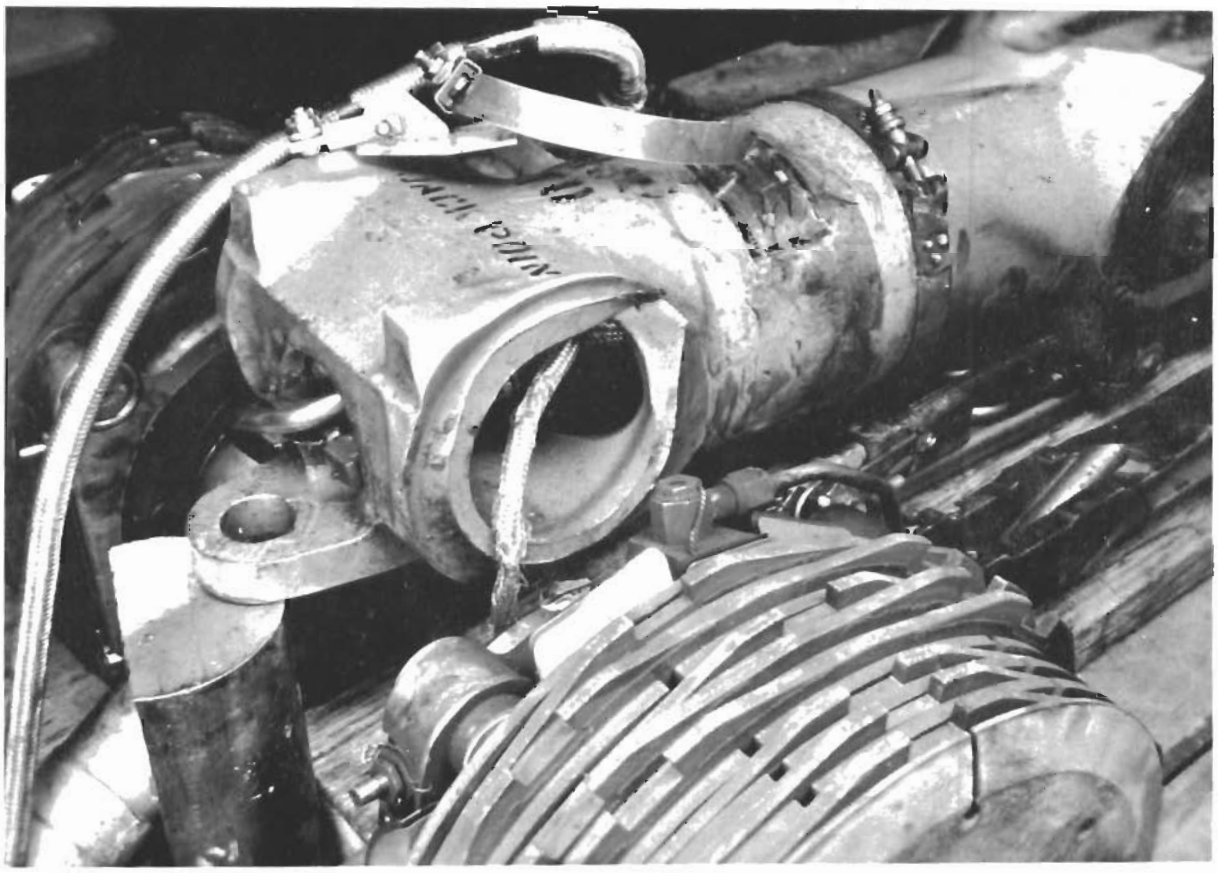

Figure 27. Axle Beam Failure 11/61 AISI 4340 (260-280 ksi UTS)

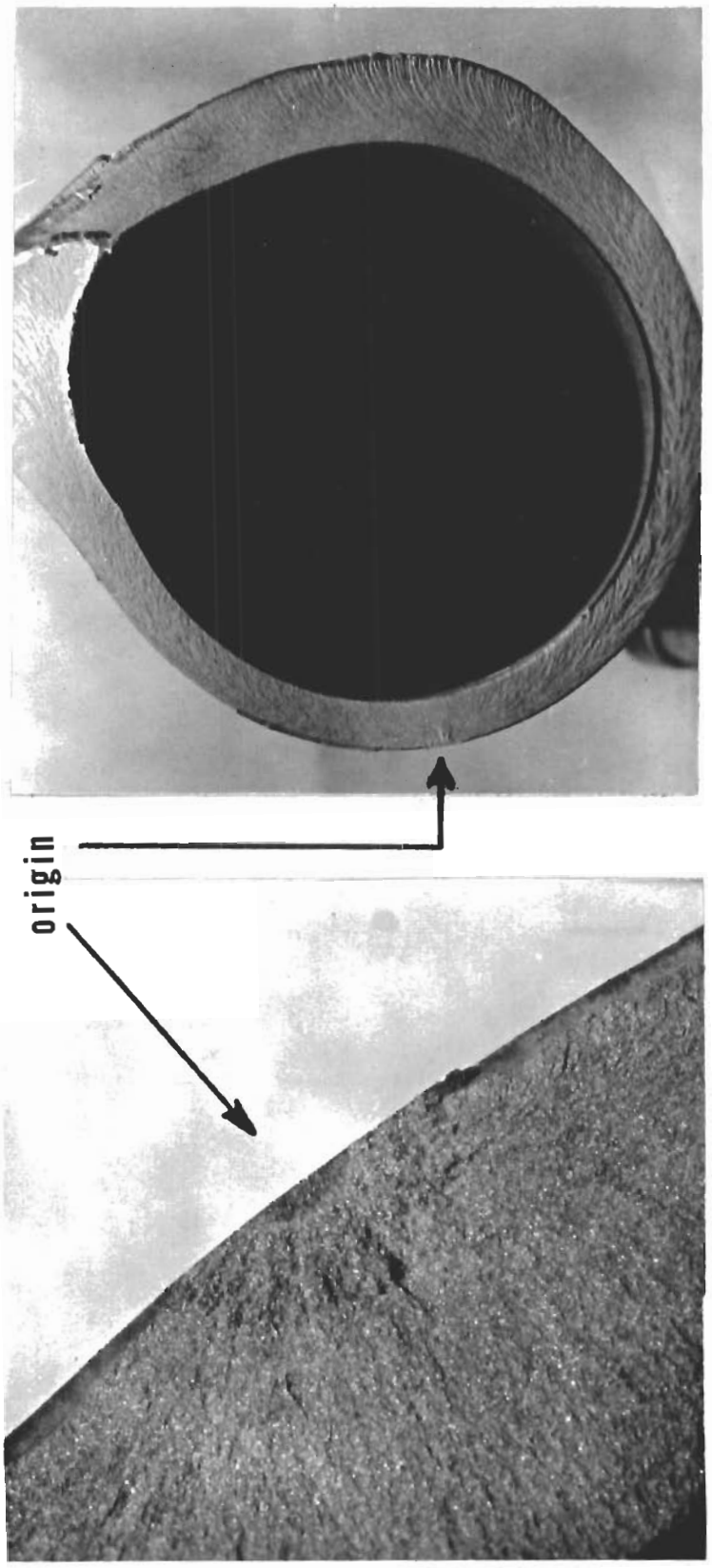

Figure 28. Fracture Origin - Axle Beam Failure 11/61

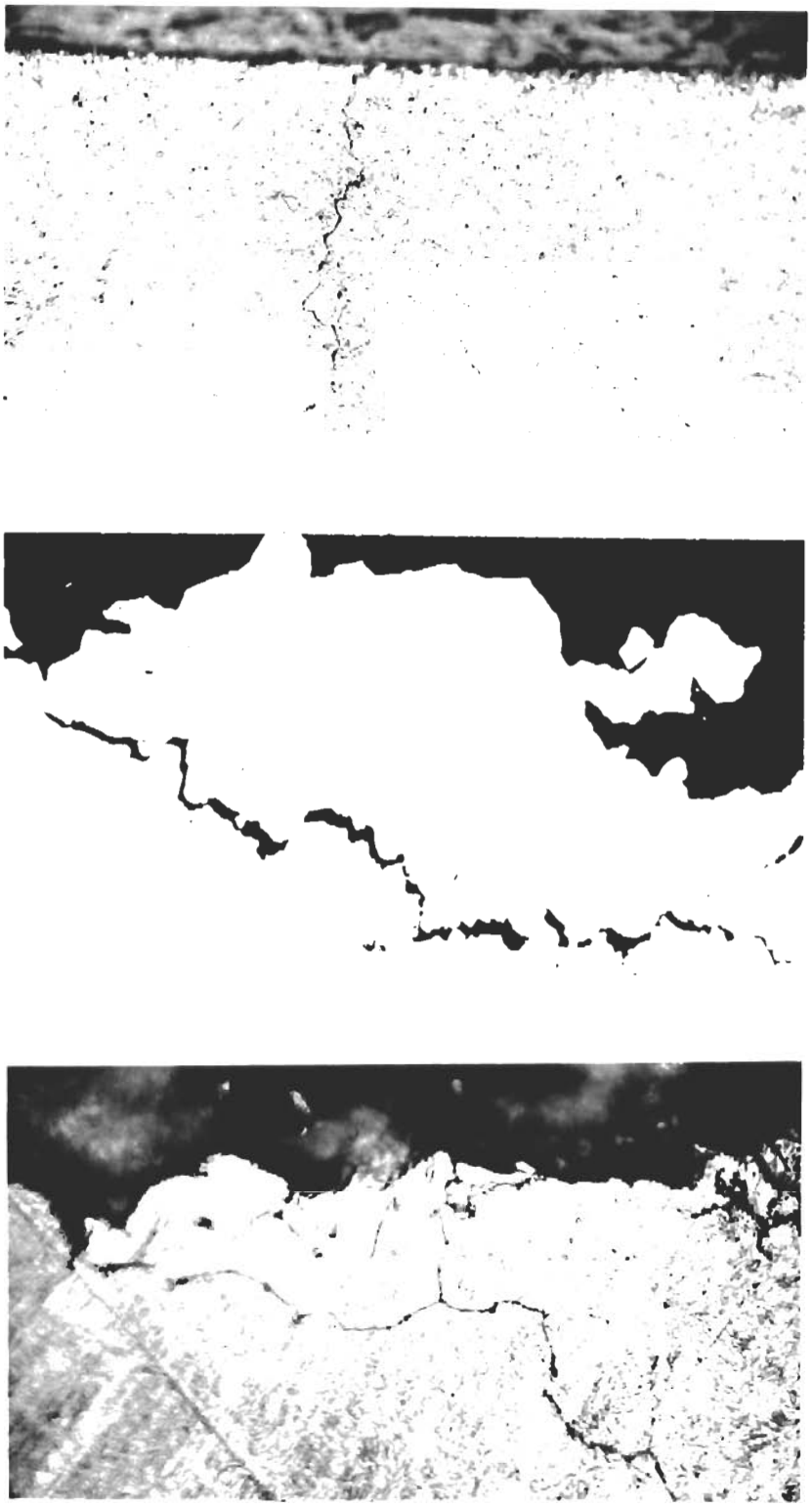

Figure 29. Intergranular Cracking - Axle Beam Failure

APPROXIMATELY 10,000 X

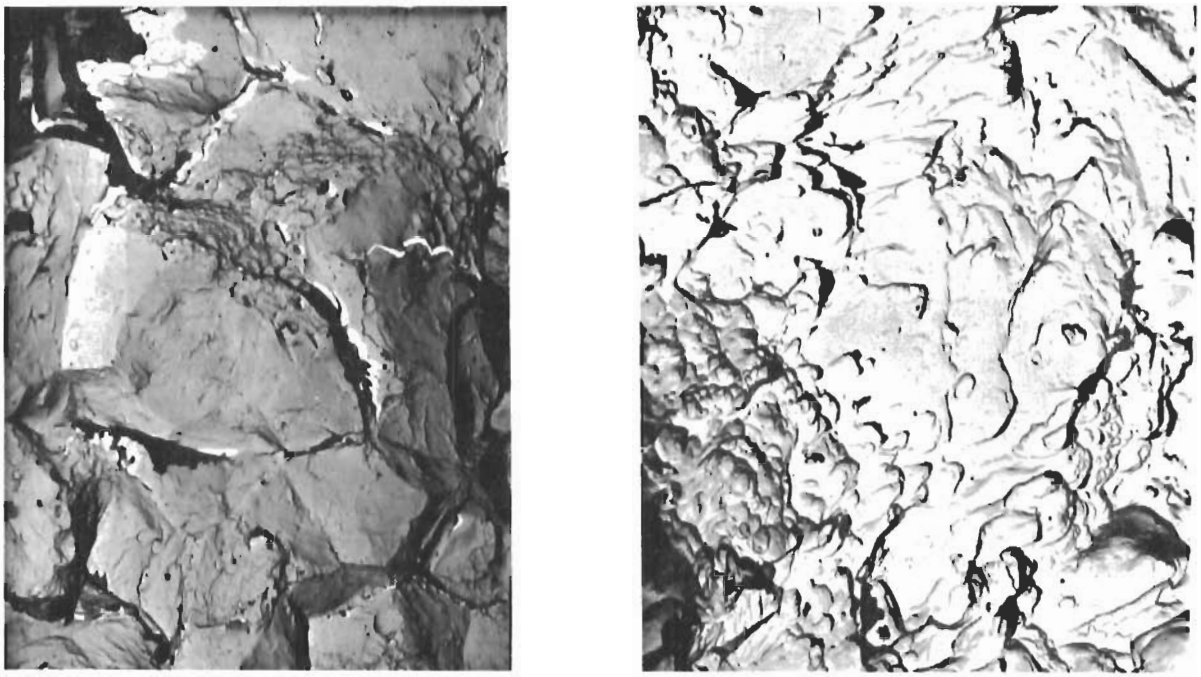

(A) FAILURE ORIGIN (INTERGRANULAR)

(B) DUCTILE FRACTURE

Figure 30. Electron Fractographs of Primary Axle Beam Failure

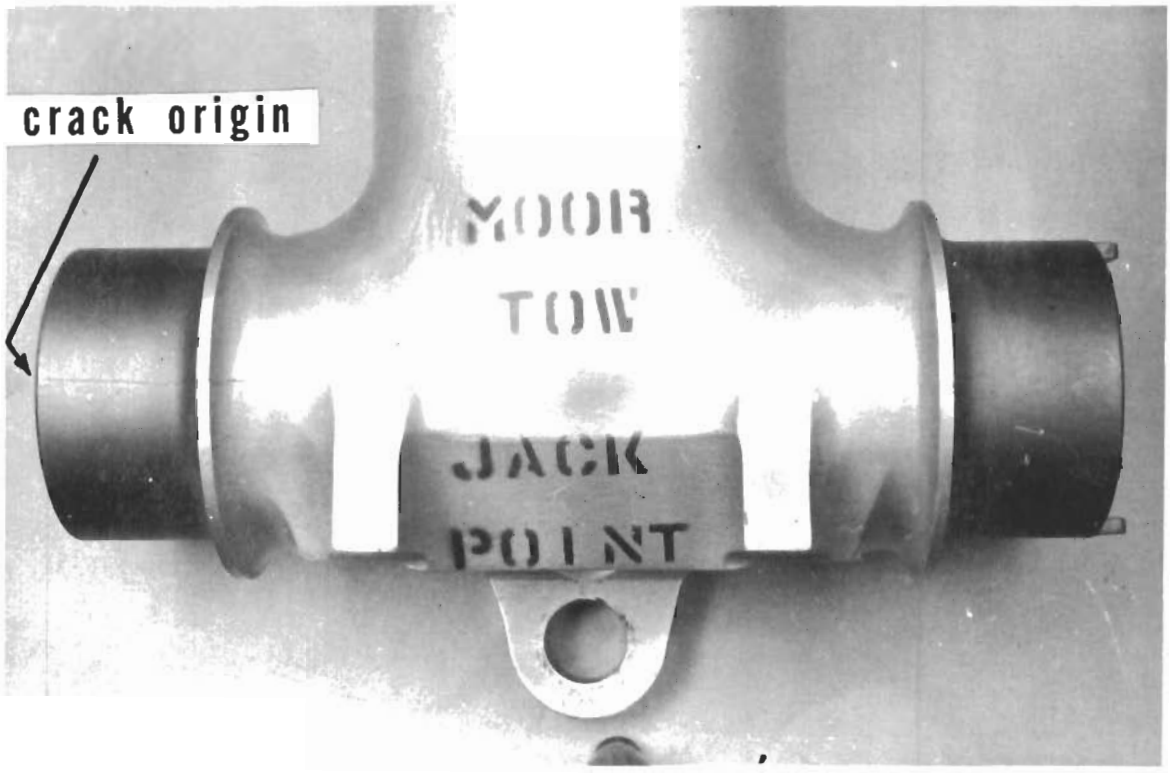

Figure 31. Axle Beam Failure Through Axle Design 1/62 AISI 4340 (260-280 ksi UTS)

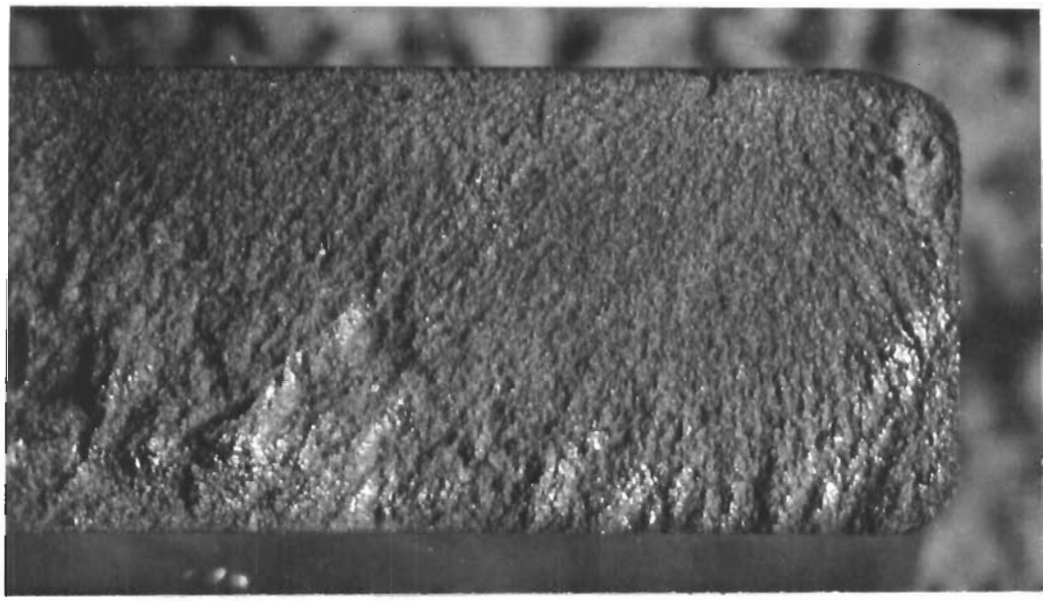

Fracture Origin

Figure 32. Axle Beam Failure 1/62

#2 INTERGRANULAR

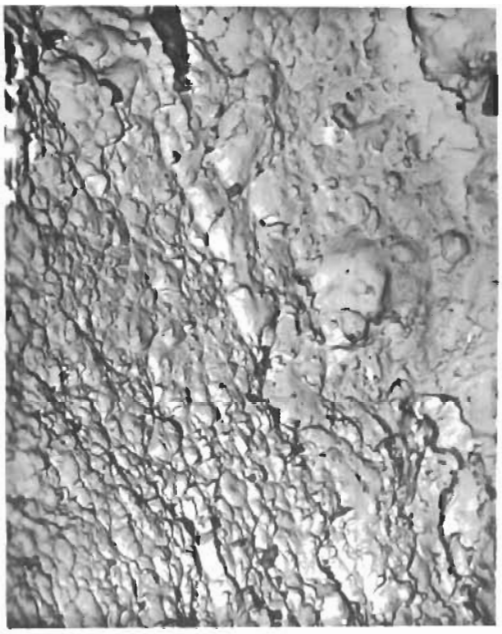

#3 DUCTILE

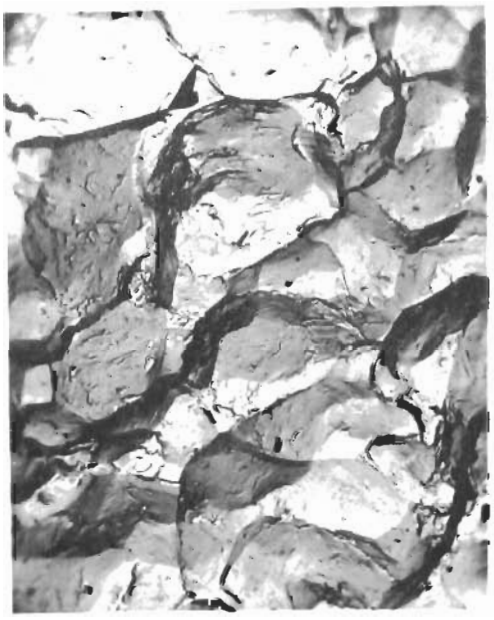

#1 INTERGRANULAR

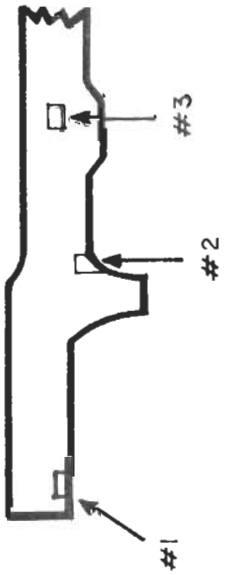

SPECIMEN LOCATION

Figure 33. Axle Beam Failure

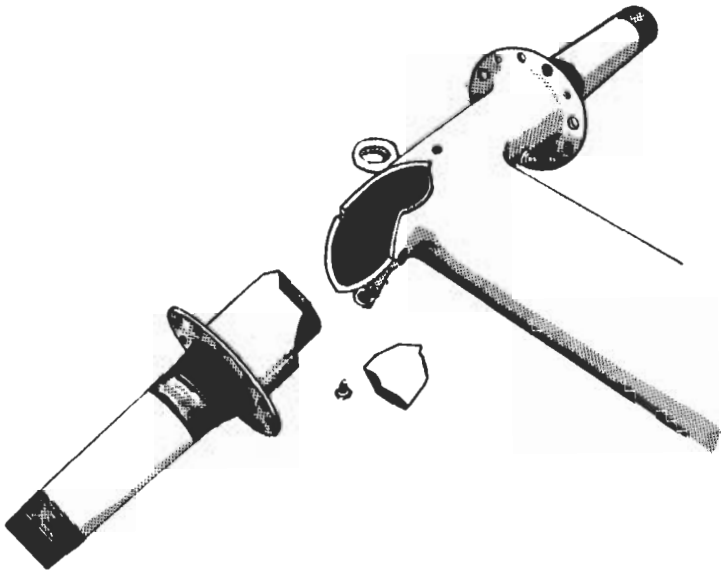

(a) Forward Gear Assembly

Origin - Forward Bolt Line

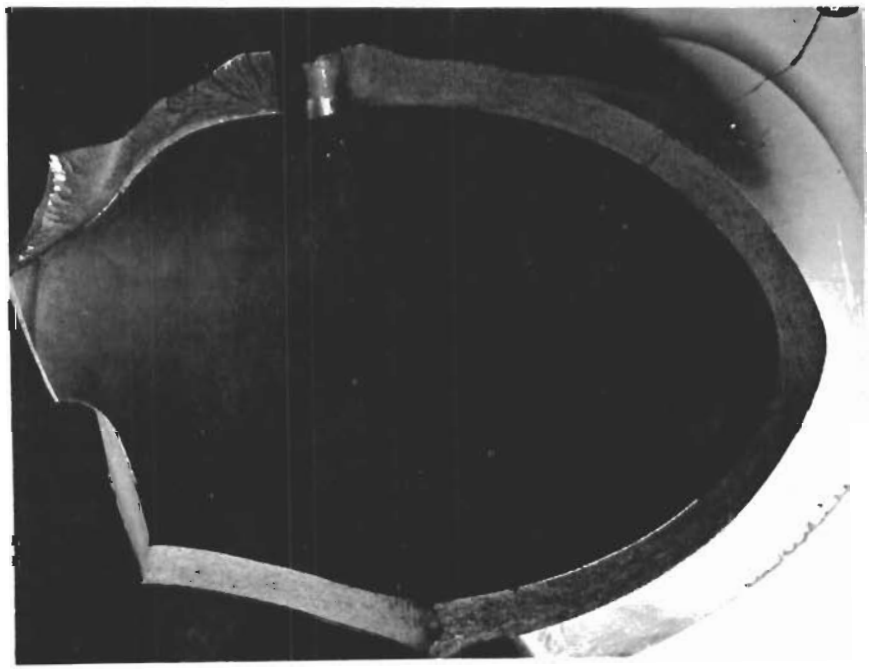

(b) Fracture Surface

Figure 34. **Landing Gear - Truck Beam Assembly Failure AISI 4340 (260-280 ksi UTS)**

(A) 2X MAGNIFICATION

(B) 5X MAGNIFICATION

(C) 175X MAGNIFICATION

FAILURE ORIGIN - MACROSCOPIC ANALYSIS

Figure 35. Landing Gear Truck Beam Failure AISI 4340 (260-280 ksi UTS)

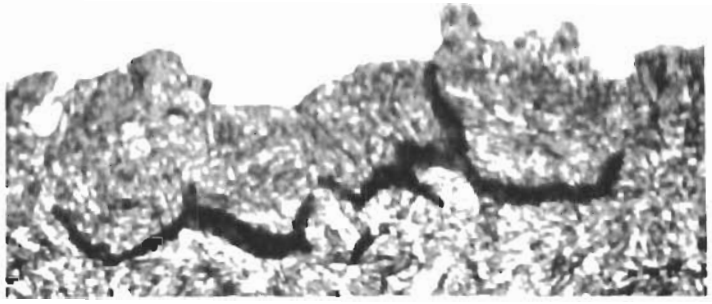

(a) 750X Nital Etch
Secondary Cracking

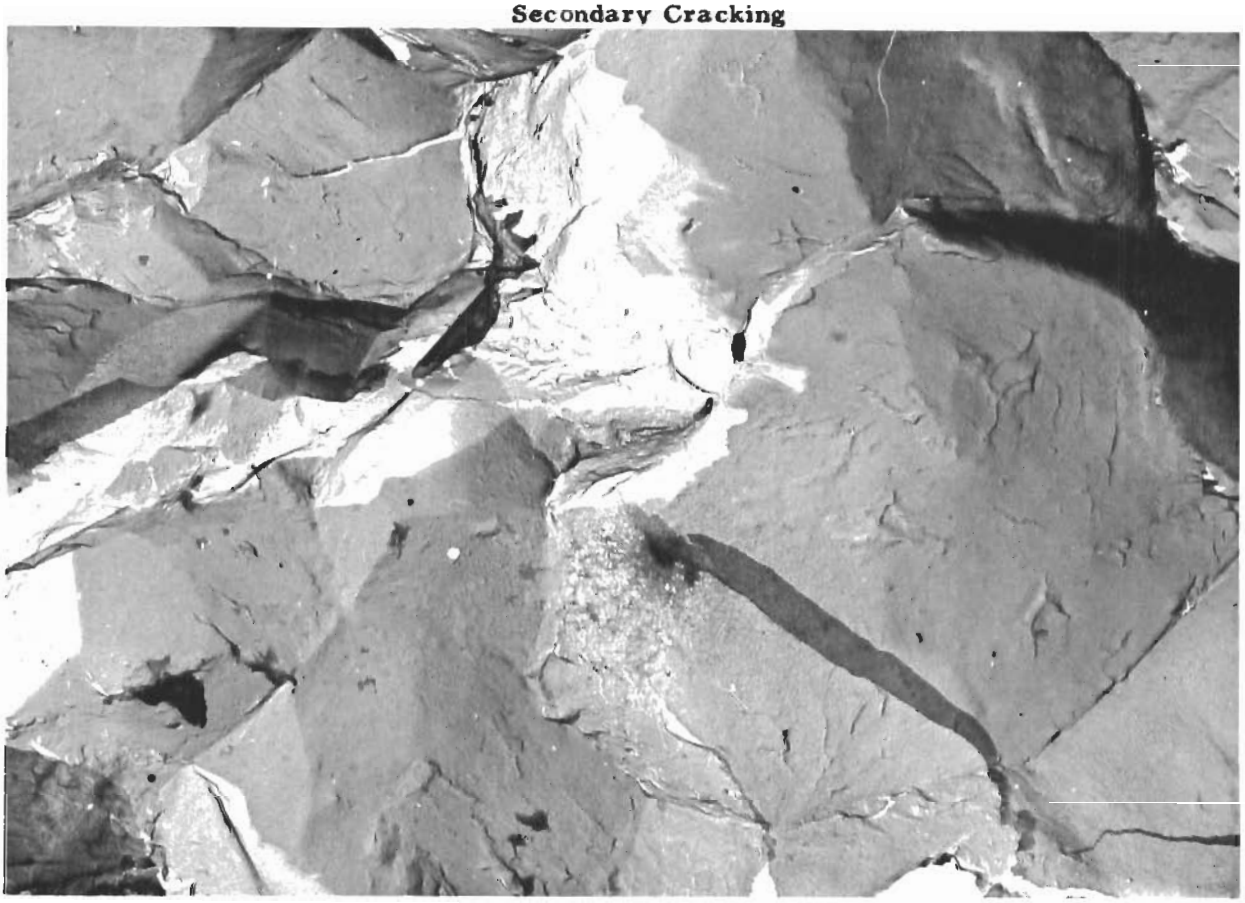

(b) X Electron Fratograph

Failure Origin - Microscopic Analysis

Figure 36. Landing Gear Truck Beam Failure AISI 4340 (260-280 ksi UTS)